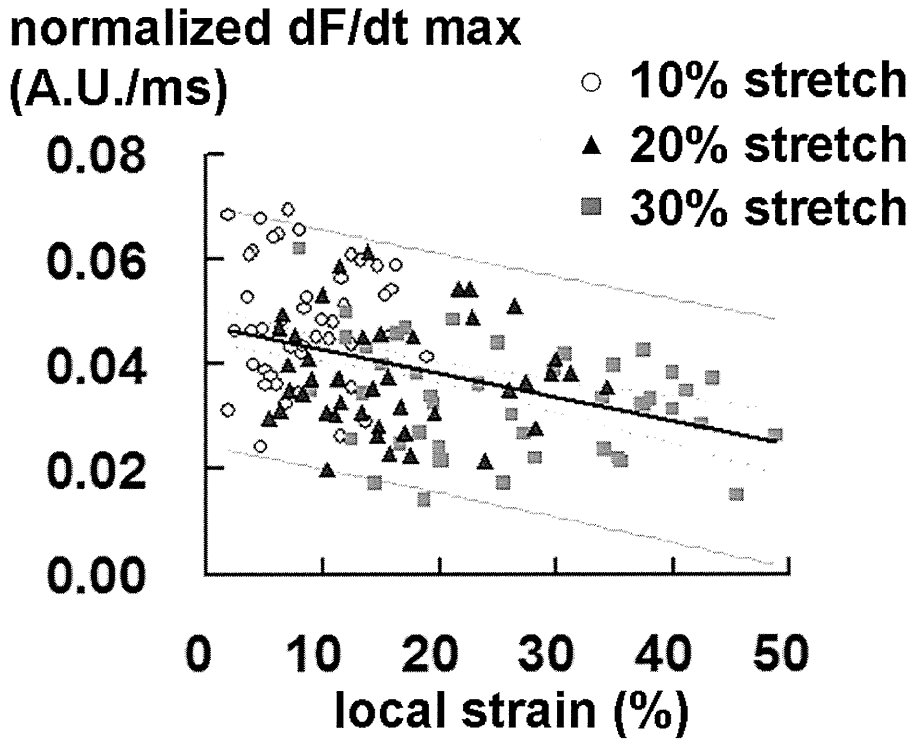

Online Figure VII

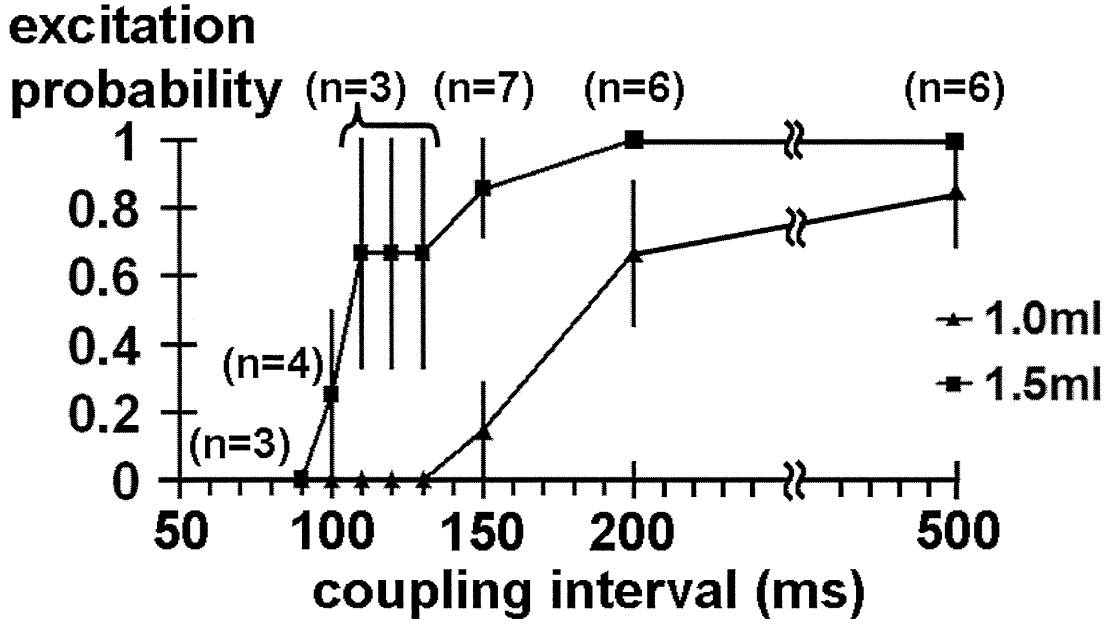

Online Figure VIII

J Physiol Sci
DOI 10.1007/s12576-010-0086-y

ORIGINAL PAPER

Right ventricular stiffness constant as a predictor of postoperative hemodynamics in patients with hypoplastic right ventricle: a theoretical analysis

Shuji Shimizu · Toshiaki Shishido · Dai Une · Atsunori Kamiya · Toru Kawada · Shunji Sano · Masaru Sugimachi

Received: 9 December 2009 / Accepted: 10 January 2010

Abstract One and a half ventricle repair (1.5VR) is a surgical option for hypoplastic right ventricle (RV). The benefits of this procedure compared to biventricular repair (2VR) or Fontan operation remain unsettled. To compare postoperative hemodynamics, we performed a theoretical analysis using a computational model based on lumped-parameter state-variable equations. We varied the RV stiffness constant (B_{RV}) to simulate the various RV hypoplasia, and estimated hemodynamics for a given B_{RV}. With $B_{RV} < 150\%$ of normal, cardiac output was the largest in 2VR. With $B_{RV} > 150\%$, cardiac output became larger in 1.5VR than in 2VR. With $B_{RV} > 250\%$, RV end-diastolic volume was almost the same between 1.5VR and 2VR, and a rapid increase in atrial pressure precluded the use of 1.5VR. These results indicate that the beneficial effect of 1.5VR depends on the RV stiffness constant. Determination of management strategy should not only be based on the morphologic parameters but also on the physiological properties of RV.

S. Shimizu (✉) · T. Shishido · D. Une · A. Kamiya · T. Kawada · M. Sugimachi
Department of Cardiovascular Dynamics, Advanced Medical Engineering Center, National Cardiovascular Center Research Institute, 5-7-1 Fujishiro-dai, Suita, Osaka 565-8565, Japan
e-mail: shujismz@ri.ncvc.go.jp

S. Shimizu · S. Sano
Department of Cardiovascular Surgery, Okayama University Graduate School of Medicine, Dentistry and Pharmaceutical Sciences, Okayama, Japan

S. Shimizu
Japan Association for the Advancement of Medical Equipment, Tokyo, Japan

Keywords One and a half ventricle repair · Right ventricular stiffness · Hypoplastic right ventricle · Computational model

Introduction

One and a half ventricle repair (1.5VR) is a surgical option for hypoplastic right ventricle (RV) caused by various congenital heart diseases including pulmonary atresia with intact ventricular septum (PA/IVS), Ebstein's anomaly or their relatives. In this procedure, the superior vena cava (SVC) is directly connected to the pulmonary artery (PA). Therefore, the blood from SVC directly enters PA, whereas the blood from the inferior vena cava (IVC) is pumped by RV to PA. This procedure is clinically acceptable because of its low surgical risk [1, 2]. However, the benefits of this procedure on postoperative hemodynamics in patients with a wide spectrum of RV hypoplasia compared to other procedures such as biventricular repair (2VR) and Fontan operation remain unsettled [3]. Furthermore, conversion to Fontan circulation was required late after 1.5VR in a possibly inappropriate candidate [4].

Although various authors reported an arbitrary selection scheme for the procedures based on RV morphology such as RV end-diastolic volume (RVEDV) [1, 2, 5], the long-term outcomes of 1.5VR have remained insufficiently known [5]. The previous criteria do not likely predict postoperative hemodynamics of these complex circulations accurately because morphological values measured preoperatively largely depend on the RV preload and afterload conditions, which change remarkably between subjects and between before and after the operation.

Hypoplastic RV is physiologically characterized by increased RV stiffness, caused by hypertrophy and

Published online: 04 February 2010

fibroelastosis of RV muscles [6]. However, how RV stiffness influences the postoperative hemodynamics has not been reported. Given the small number of patients with each of the wide variety of preoperative RV conditions [7, 8], the influence of RV stiffness on 1.5VR, 2VR, and Fontan operation cannot be examined by clinical study. It is also difficult to experimentally reproduce hemodynamics before and after 1.5VR for hypoplastic RV with various stiffness. In view of the above, we attempted to clarify postoperative hemodynamics by a theoretical analysis using a computational model based on lumped-parameter state-variable equations. The present results indicate that the RV stiffness constant may provide selection criteria for 1.5VR.

Materials and methods

The electrical analogs of the model used to simulate the cardiovascular system are shown in Fig. 1. We modeled the postoperative cardiovascular system mathematically by a combination of the time-varying elastance cardiac chamber model and the three-element Windkessel vascular model. We set the normal values of parameters to be appropriate for a 75-kg man. These values were obtained from the literature [9–13] and are listed in Table 1. Since the data of the pressure–volume relationship of the atrium were scarcely available, parameters of the atrium were surmised from the literature [10–12].

Heart

The right and left ventricular chambers as well as the atrial chambers are represented by the time-varying elastance model [9, 10, 13]. The end-systolic pressure–volume relationship is described by a linear formula:

$$P_{es,cc} = E_{es,cc}\left[V_{es,cc} - V_{0,cc}\right] \quad (1)$$

where $P_{es,cc}$ and $V_{es,cc}$ are end-systolic pressure and volume, respectively; $E_{es,cc}$ is the maximal volume elastance; $V_{0,cc}$ is the volume at which $P_{es,cc}$ is equal to 0 mmHg. cc denotes each chamber, i.e., RA for the right atrium, LA for the left atrium, RV for the right ventricle, or LV for the left ventricle. The end-diastolic pressure–volume relationship is represented by a non-linear formula:

$$P_{ed,cc} = A_{cc}\left[e^{B_{cc}(V_{ed,cc}-V_{0,cc})} - 1\right] \quad (2)$$

where $P_{ed,cc}$ and $V_{ed,cc}$ are end-diastolic pressure and volume, respectively; A_{cc} and B_{cc} are constants [9, 10, 13]. We assumed the time course of the time-varying elastance by defining normalized elastance curve $e_{cc}(t)$ as:

Table 1 Parameters used in modeling

Heart rate (HR), beats/min	75			
Duration of cardiac cycle (T_c), ms	800			
Time advance of atrial systole (DT), ms	16			
Total stressed blood volume (V_s), ml	750	(control only)		
	LV	RV	LA	RA
Time to end systole (T_{es}), ms	200	200	120	120
End-systolic elastance (E_{es}), mmHg/ml	3.0	0.7	0.5	0.5
Scaling factor of EDPVR (A), mmHg	0.35	0.35	0.06	0.06
Exponent scaling factor for EDPVR (B), ml^{-1}	0.033	0.023	0.264	0.264
Unstressed volume (V_0), ml	0	0	5	5
	Aortic	Pulmonary	Mitral	Tricuspid
Valvular resistance (forward), (mmHg s)/ml	0.001	0.001	0.001	0.001
	Systemic		Pulmonary (p)	
	Superior (ss)	Inferior (si)		
Arterial resistance (R_a), (mmHg s)/ml	2.25	1.5	0.03	
Characteristic impedance (R_c), (mmHg s)/ml	0.075	0.05	0.02	
Venous resistance (R_v), (mmHg s)/ml	0.0375	0.025	0.015	
Arterial capacitance (C_a), ml/mmHg	0.528	0.792	13	
Venous capacitance (C_v), ml/mmHg	28	42	8	

LV Left ventricle, *RV* right ventricle, *LA* left atrium, *RA* right atrium, *EDPVR* end-diastolic pressure–volume relationship

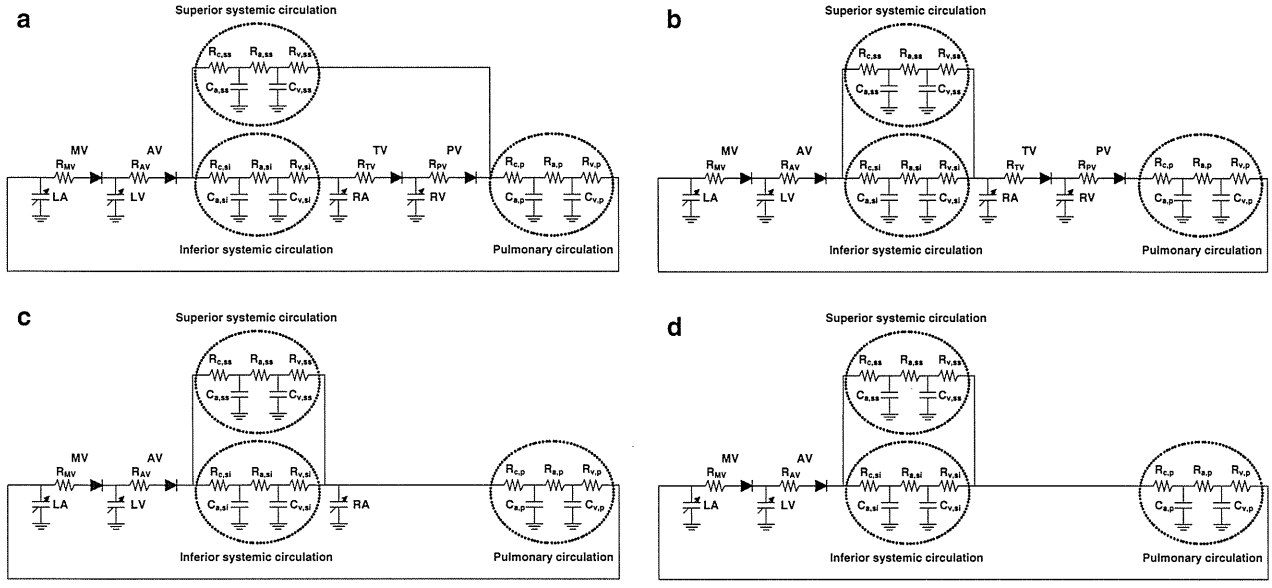

Fig. 1 **a** The electric equivalent circuit of one and a half ventricle repair. **b** Biventricular repair (normal circulation). **c**,**d** Variations of Fontan operation [**c** atriopulmonary connection (APC); **d** total cavopulmonary connection (TCPC)]. *LV* and *RV* left and right ventricles, *LA* and *RA* left and right atria, *AV* and *MV* aortic and mitral valves, *PV* and *TV* pulmonary and tricuspid valves, C_a and C_v lumped arterial and venous capacitances, R_c characteristic impedances, R_a lumped arterial resistances, R_v venous resistances, *ss* superior systemic circulation, *si* inferior systemic circulation, *p* pulmonary circulation

$$\begin{aligned} e_{cc}(t) &= 0.5[1-\cos(\pi t/T_{es,cc})]\ (0 \le t < 2T_{es,cc}) \\ e_{cc}(t) &= 0\ (2T_{es,cc} \le t < T_c) \end{aligned} \quad (3)$$

where t is the time from the start of systole, $T_{es,cc}$ is the duration of systole, and T_c is the duration of cardiac cycle. Using $e_{cc}(t)$, the instantaneous pressure, $P_{cc}(t)$, is described by:

$$P_{cc}(t) = [P_{es,cc}(V_{cc}) - P_{ed,cc}(V_{cc})]e_{cc}(t) + P_{ed,cc}(V_{cc}) \quad (4)$$

Ventricular systole is preceded by atrial systole. The time advance of atrial systole (DT) is calculated as the fixed fraction of T_c ($DT = 0.02T_c$). Function of each chamber is characterized by the parameters $E_{es,cc}$, $T_{es,cc}$, $V_{0,cc}$, A_{cc}, B_{cc}, and $e_{cc}(t)$. The same $e_{cc}(t)$ was used for all chambers, but the other parameters were different between chambers, as shown in Table 1.

Vascular system

Basically, the pulmonary and systemic circulations are modeled as modified Windkessel impedances. Each vascular system is modeled by lumped venous (C_v) and arterial (C_a) capacitances, a characteristic impedance (R_c) that is related to the stiffness of the proximal aorta or pulmonary artery, a lumped arterial resistance (R_a), and a resistance proximal to C_v (R_v). This framework is similar to that used in deriving Guyton's resistance to venous return [14].

To simulate the postoperative hemodynamics of 1.5VR, the systemic circulation is divided into two parts, the superior and the inferior circulation. Therefore, the parameters of the systemic circulation are also divided into the superior and inferior ones, as shown in Fig. 1. Blood flow in the descending aorta is reported to be 63.8% of the left ventricular output [15]. The compliance of the IVC is considered to be 66.6% of the total venous compliance [16]. Thus, in our model, arterial and venous compliances of the inferior systemic circulation are adjusted to 0.6 times those of the compliance of the total circulation, and the blood flow of the inferior systemic circulation is controlled to be 60% of the left ventricular output by adjusting the resistances of R_c, R_a, and R_v.

The capacitance of the superior systemic circulation is also divided into arterial ($C_{a,ss}$) and venous ($C_{v,ss}$). Similarly, arterial and venous capacitances are defined for the inferior systemic circulation ($C_{a,si}$ and $C_{v,si}$) and for the pulmonary circulation ($C_{a,p}$ and $C_{v,p}$). The ratio of C_a to C_v was obtained from the literature [9, 10, 13]. The relationship between pressure (P_c) and volume (V_c) in each capacitance is described by the following linear formula.

$$P_c = \frac{V_c}{C} \quad (5)$$

The changes in volume in each capacitance ($dV(t)/dt$) are described by the differential equations below

$$\frac{dV(t)}{dt} = \sum Q_{\text{in-flow}}(t) - \sum Q_{\text{out-flow}}(t) \quad (6)$$

where $\Sigma Q_{\text{in-flow}}(t)$ and $\Sigma Q_{\text{out-flow}}(t)$ indicate the sum of instantaneous volumetric flow rates at the inlet and outlet of each compartment, respectively. Each of the aortic, mitral, pulmonary, and tricuspid valves is described as an ideal diode with a serially connected small resistor.

In the 1.5VR model, the superior circulation flows from SVC to PA, while the inferior blood flow returns to RA through IVC as shown in Fig. 1a. The models of 2VR (Fig. 1b) and variations of Fontan operation [Fig. 1c, atriopulmonary connection (APC); Fig. 1d, total cavopulmonary connection (TCPC)] are constructed for comparisons. Although the superior and inferior systemic circulations return to RA in both 2VR and APC models, RA is directly connected to PA in the APC model. In the TCPC model, SVC and IVC are directly connected to PA. All parameter values were the same for all of these models except total stressed blood volume (see below) (Table 1).

Hypoplastic RV

Hypoplastic RV is physiologically characterized by an increase in RV stiffness caused by hypertrophy and fibroelastosis of RV muscles [6]. Recalling Eq. 2 for RV, we have:

$$P_{\text{ed,RV}} = A_{\text{RV}}\left[e^{B_{\text{RV}}\left(V_{\text{ed,RV}} - V_{0,\text{RV}}\right)} - 1\right] \quad (7)$$

where B_{RV} is stiffness constant of RV. The value of B_{RV} was changed stepwise from 0.023/ml (normal RV) to 0.143/ml (extremely stiff RV) in increments of 0.01/ml to simulate the various degrees of RV stiffness associated with hypoplasia (Fig. 2).

Protocols

First, the control state was simulated by the 2VR model with normal RV stiffness constant ($B_{\text{RV}} = 0.023$). The total stressed blood volume (V_s), equal to the sum of the stressed volumes in each capacitance and the volume of each chamber, was set as 750 ml to reproduce normal hemodynamics.

$$V_s = V_{\text{LV}} + V_{\text{RV}} + V_{\text{LA}} + V_{\text{RA}} + V_{\text{Ca,ss}} + V_{\text{Cv,ss}} + V_{\text{Ca,si}} + V_{\text{Cv,si}} + V_{\text{Ca,p}} + V_{\text{Cv,p}} \quad (8)$$

We solved these simultaneous equations (Eqs. 1–8) using the component ODE45 of MATLAB, based on the Runge–Kutta method (MathWorks). The hemodynamic parameters of 2VR with normal RV stiffness constant are listed in Table 2.

Next, systemic cardiac output, pulmonary arterial pressure (PAP), right atrial pressure (RAP), and RVEDV after each procedure were calculated for each RV stiffness constant. Heart rate was kept constant and mean systemic arterial pressure (MAP) was controlled at the same value as that of the control state, by adjusting the total stressed blood volume.

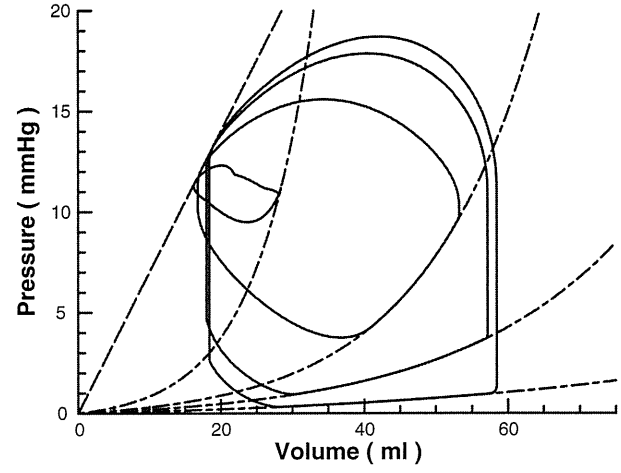

Fig. 2 Right ventricular pressure–volume loops (PV loop) after one and a half ventricle repair. With the increase in the right ventricular stiffness constant, the PV loop became smaller. The *horizontal axis* is the instantaneous right ventricular volume (ml) and the *longitudinal axis* is the instantaneous right ventricular pressure (mmHg)

Table 2 Control hemodynamic parameters (2VR with normal RV stiffness constant)

Parameter	Value
Heart rate (HR), beats/min	75
Mean systemic arterial pressure (MAP), mmHg	80.3
Mean pulmonary arterial pressure (PAP), mmHg	13.6
Mean right atrial pressure (RAP), mmHg	2.34
Mean left atrial pressure (LAP), mmHg	8.26
Left ventricular cardiac output (CO), l/min	4.95

Results

Figure 3a shows the impact of the RV stiffness constant on systemic cardiac output after each procedure. In the Fontan circulation (APC and TCPC), systemic cardiac output was independent of the RV stiffness constant and remained at 4.40 l/min. Under the condition of normal RV stiffness constant, systemic cardiac output was 4.95 l/min in 2VR and 4.73 l/min in 1.5VR, being 13 and 8% greater than that of Fontan circulation, respectively. As the RV stiffness constant was increased from the control value to mimic increased severity of RV

hypoplasia, systemic cardiac output decreased in both 2VR and 1.5VR circulations. Within the range between 100 and 150% of the control RV stiffness constant, systemic cardiac output of 2VR circulation was obviously greater than those of other two circulations. With the RV stiffness constant >150%, systemic cardiac output became greater in 1.5VR than in 2VR. In this situation, 2VR needed larger stressed blood volume than 1.5VR to maintain MAP (Fig. 3d).

The results for PAP and RAP are shown in Fig. 3b. As the RV stiffness constant increased, PAP decreased and RAP increased in both 2VR and 1.5VR circulations. In 2VR circulation, RAP increased steeply as the RV stiffness constant increased up to 150% of normal, and exceeded the atrial pressure of TCPC when the RV stiffness constant increased above 150% of normal. In 1.5VR circulation, RAP also increased but more slowly and exceeded the atrial pressure of TCPC only when the RV stiffness constant increased above 250% of normal. PAP in 1.5VR circulation, which was equal to SVC pressure, became higher than PAP in 2VR circulation in the range of RV stiffness constant >150% of normal.

In the control state, RVEDV in 2VR was 87.7 ml, which was treated as the value of 100% of RVEDV. The influence of the RV stiffness constant on RVEDV is shown in Fig. 3c. In 2VR circulation, RVEDV decreased as the RV stiffness constant increased. In 1.5VR circulation, RVEDV reduced only slightly with an increase in the RV stiffness constant until 250% of normal. In the range of RV stiffness constant >250% of normal, RVEDV showed a relatively linear decay in both 2VR and 1.5VR circulations, and there was no difference in RVEDV between 2VR and 1.5VR. In this situation, both 1.5VR and 2VR needed larger stressed blood volume than Fontan circulation (Fig. 3d).

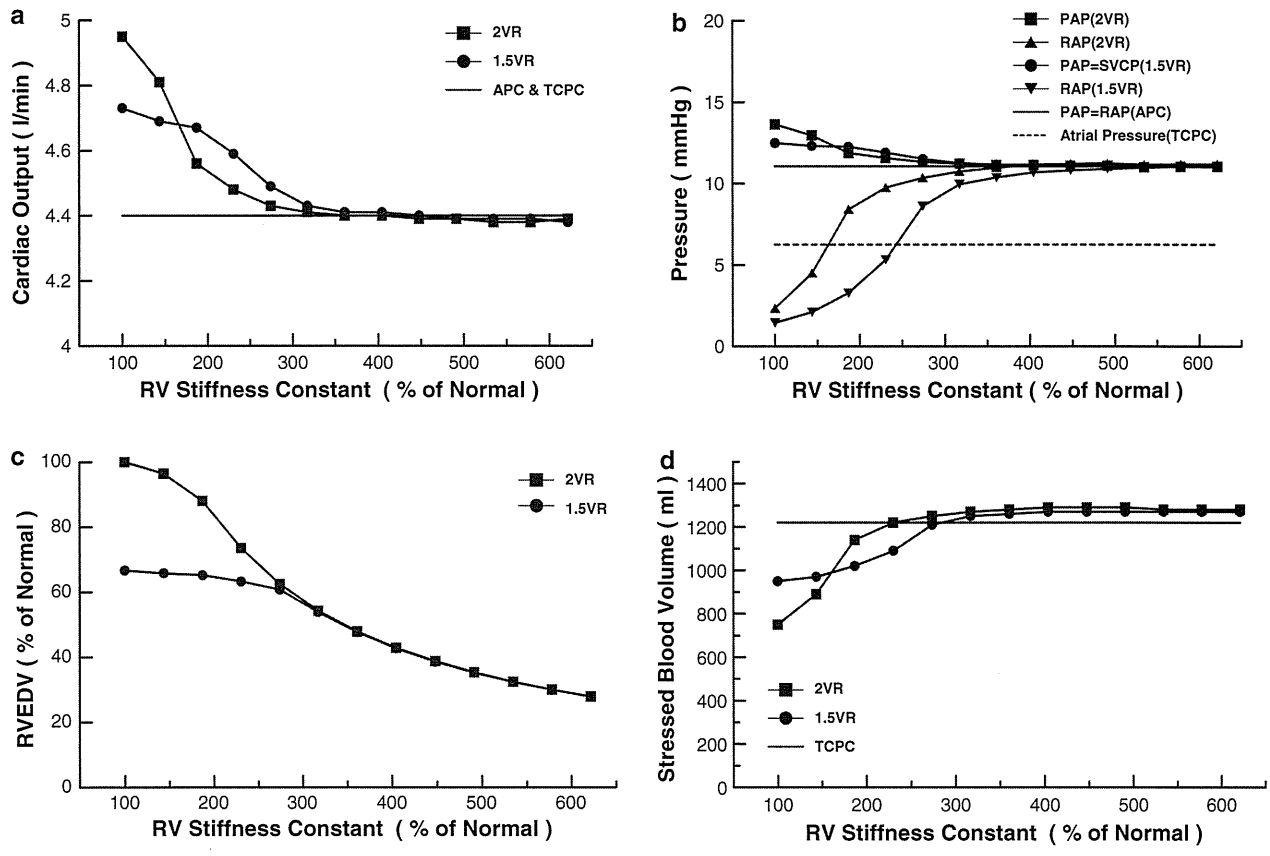

Fig. 3 **a** The relationship between systemic cardiac output (l/min) and % stiffness constant of hypoplastic right ventricle. The *horizontal axis* is the ratio of RV stiffness constant (% stiffness constant) to the normal value. **b** The relationship between pulmonary arterial pressure or right atrial pressure (mmHg) and % stiffness constant of hypoplastic RV. Pulmonary arterial pressure is the same as right atrial pressure in APC. **c** The relationship between % RVEDV and % stiffness constant of hypoplastic RV. **d** The relationship between stressed blood volume (ml) and % stiffness constant. *2VR* biventricular repair, *1.5VR* one and a half ventricle repair, *APC* and *TCPC* variations of Fontan operation (*APC* atriopulmonary connection, *TCPC* total cavopulmonary connection); *PAP* pulmonary arterial pressure, *RAP* right atrial pressure, *SVCP* superior vena caval pressure, *RVEDV* right ventricular end-diastolic volume

Discussion

The results of this theoretical analysis suggest that, in patients with hypoplastic RV, postoperative hemodynamics depends largely on the RV stiffness constant. PA/IVS, Ebstein's anomaly or their relatives are characterized by varying degrees of underdevelopment of RV. For a severely hypoplastic RV, the definitive treatment is single ventricular circulation. For a mildly hypoplastic RV, biventricular circulation is expected to have merit. Recently, 1.5VR has been proposed to reduce the surgical risk of 2VR. The use of 1.5VR has lowered the early or midterm mortality, and adequate growth of RV and the tricuspid valve has been documented in some patients [2]. However, the postoperative RV dysfunction or arrhythmic event has also been reported, in particular, when the patients are on the borderline of criteria between 1.5VR and Fontan operation [4, 5].

For the choice of surgical options among Fontan operation, 1.5VR, and 2VR, the previously used criteria were based on morphologic characteristics of the hypoplastic RV, such as RVEDV. However, simple anatomic indices may be inaccurate, since these values are dependent on the afterload and preload conditions. For that reason, the treatment strategy for hypoplastic RV based on the anatomic indices remains controversial. We focused on the intrinsic property of hypoplastic RV, i.e., RV stiffness constant. The fact that the RV stiffness constant, an index of chamber property, is relatively independent of the loading condition is important for the accurate prediction of postoperative hemodynamics. Based on the results of the present study, we propose that patients with hypoplastic RV can be classified into three groups according to the RV stiffness constant. The first group consists of patients with mild RV hypoplasia (RV stiffness constant <150% of normal), in whom enlargement of RV is expected after the operation. At the other extreme, the second group consists of patients with severe RV hypoplasia (RV stiffness constant >250%), in whom no RV reconstruction is expected to have merit. In addition, we have shown that there certainly exists a third group consisting of patients with intermediate RV hypoplasia (RV stiffness constant between 150 and 250%), who would benefit more from 1.5VR than from 2VR or Fontan operation.

Mild RV hypoplasia

When RV hypoplasia is mild (RV stiffness constant <150% of normal), systemic cardiac output is greater in 2VR than in 1.5VR or Fontan operation (APC or TAPC). Therefore, we recommend that 2VR should be chosen in the mild RV hypoplasia group. Although systemic cardiac output in 1.5VR is also greater than that in Fontan operation, SVC pressure (which is equal to PAP) is higher than that of APC. Accordingly, the upper part of the body is exposed to higher SVC pressure in 1.5VR, which may cause postoperative pleural effusion [2]. A large pressure gradient between SVC and IVC also results in abnormal venous collaterals from SVC to IVC [17–20], and they could effectively increase the venous return to RA in 1.5VR.

Intermediate RV hypoplasia

When RV hypoplasia is intermediate (RV stiffness constant between 150 and 250% of normal), systemic cardiac output in 1.5VR exceeds that in 2VR. Although SVC pressure is still higher in 1.5VR than in APC, RAP is lower in 1.5VR than in the other procedures. This condition is favorable to reduce supraventricular arrhythmias related to high RAP during the perioperative periods. This beneficial effect is not expected for 2VR since RAP in 2VR is higher than the atrial pressure of TCPC. Furthermore, 1.5VR is advantageous from the viewpoint of stressed blood volume because 1.5VR needs smaller stressed blood volume than does 2VR to maintain MAP (Fig. 3d).

In these patients, RVEDV in 1.5VR is relatively independent of the RV stiffness constant. However, abnormal systemic venous collateral channels might open after 1.5VR. These collateral channels would increase RV preload wastefully and decrease systemic cardiac output in the late postoperative phase. In such conditions, conversion to the Fontan circulation may be required in the late phase [4, 5]. Nevertheless, 1.5VR should be recommended for the intermediate RV hypoplasia group because high cardiac output and low RAP are anticipated.

Severe RV hypoplasia

When RV hypoplasia is severe (RV stiffness constant >250% of normal), neither 1.5VR and 2VR are expected to improve systemic cardiac output. In this condition, RVEDV is almost the same between 1.5VR and 2VR, and linearly decreases with an increase in the RV stiffness constant in spite of a rapid elevation in RAP. This indicates that RVEDV might be independent of the venous return to RA. Since RAP becomes higher than the atrial pressure of TCPC even in 1.5VR, supraventricular arrhythmias caused by high RAP are liable to occur [2, 5]. In this condition, 1.5VR is considered to have hemodynamics equivalent to APC and needs larger stressed blood volume than does TCPC to maintain systemic arterial pressure (Fig. 3d).

Therefore, TCPC should be chosen for patients with severe RV hypoplasia. In these patients, the arrhythmic events after TCPC are less than that after APC [21, 22]. Although a small pressure gradient between SVC and IVC

remains in 1.5VR, this may not be of clinical significance. Systemic venous collateral channels are expected to be rare, and an increase of RV volume after the operation is unlikely.

Clinical implication

The management strategy for patients with hypoplastic RV has been based on the morphological characteristics, which are dependent on the loading conditions. In contrast, we used a relatively load-independent index, RV stiffness constant, and simulated the postoperative hemodynamics. As a result, we identified the characteristics of hemodynamics after each of the surgical options, and clearly defined the indications of these operations.

Moreover, our results may be useful to theoretically speculate the reason for contrasting clinical findings. Chowdhury and colleagues [2] reported that the event rate of supraventricular arrhythmia was about 15% in the late postoperative phase of 1.5VR. On the other hand, Numata et al. [5] reported higher arrhythmic event rate. In the former report, the patients had a relatively high postoperative RV volume (45–75% of predicted normal RV; Fig. 3c) and a large pressure gradient between SVC and IVC (mean 7.6 mmHg; Fig. 3b) after 1.5VR. Indeed, there was significant pleural effusion in 22.7% of patients. Our results suggest that good systemic cardiac output, low IVC pressure, and high SVC pressure after 1.5VR can be expected under a condition of a relatively small RV stiffness constant. A great difference between SVC and IVC pressures may cause pleural effusion. Therefore, patients in the former report are likely to have low RV stiffness. In the latter report, the average RVEDV at 1 year after 1.5VR was about 50% of normal and there was no obvious collateral after the surgery in the patients examined. These data suggest a high RV stiffness (Fig. 3c), and a small difference between SVC and IVC pressures (Fig. 3b). Since higher arrhythmic event rate is likely to be associated with high RAP in patients with high RV stiffness, we can interpret the marked difference in arrhythmic event rate in these studies based on postoperative hemodynamics. Operations with 1.5 VR in potentially inappropriate patients (i.e., patients with stiffer RV) might impair long-term outcomes by continued high RAP-induced arrhythmia.

If we can assess the RV stiffness constant and other hemodynamic data in a catheter laboratory before operation, we will be able to select the most suitable operation for patients with hypoplastic RV. Recently, noninvasive methods for predicting LV chamber stiffness using echocardiography have been reported [23–25]. For example, LV chamber stiffness has been estimated from the deceleration time of LV early filling, effective mitral area and length. Such a method may be applied to estimate RV chamber stiffness using the deceleration time of RV early filling, effective tricuspid area and length. Moreover, it may be possible to choose an appropriate procedure for individual patients by performing simulation of postoperative hemodynamics from individual data using our model. Further clinical studies are needed to precisely assess the RV stiffness constant, including the above methods.

Limitations

A major limitation of this study is related to the parameters we used for the model. In our model, all parameters other than the RV stiffness constant are fixed. It is reported that RV end-systolic elastance as well as the RV stiffness constant depend upon RV histological changes such as RV hypertrophy [26]. The increase in RV end-systolic elastance moves the beneficial range of 1.5VR toward the stiffer range of the RV stiffness constant. The increase of heart rate also moves the range toward the stiffer range (Table 3). Moreover, ischemia caused by long-standing hypoxemia and hypertension of RV may influence other variables [6]. The existence of pulsatility of the pulmonary circulation may also affect the pulmonary vascular resistance [27]. Tricuspid regurgitation may also impair the postoperative hemodynamics. These limitations may be solved by using the preoperative data of individual patients. Santamore and Burkhoff have already reported the importance of ventricular interdependence using a computer model [13]. However, ventricular interdependence between small hypoplastic RV and relatively large left ventricle may be negligible.

Table 3 The influence of right ventricular end-systolic elastance and heart rate on the beneficial range of the one and a half ventricle repair

	Lower limit of RV stiffness constant (% of normal)	Upper limit of RV stiffness constant (% of normal)
$E_{es,RV} = 0.7$, HR = 75	150	250
$E_{es,RV} = 1.4$, HR = 75	200	300
$E_{es,RV} = 0.7$, HR = 100	175	275

RV Right ventricle, $E_{es,RV}$ right ventricular end-systolic elastance (mmHg/ml), *HR* heart rate (beats/min)

Conclusion

Using a model analysis, we have shown that the beneficial effect of 1.5VR depends on the RV stiffness constant. 1.5VR is the most beneficial for hypoplastic RV with 150–250% of normal RV stiffness constant. The beneficial range of 1.5VR may also be changed by individual parameters other than the RV stiffness constant, but the beneficial range certainly exists. Therefore, determination of management strategy should be based not only on the morphologic parameters but also on the physiologically determined properties.

Acknowledgments This study was supported by Health and Labor Sciences Research Grants (H18-nano-Ippan-003, H19-nano-Ippan-009, H20-katsudo-Shitei-007 and H21-nano-Ippan-005) from the Ministry of Health, Labor and Welfare of Japan, by Grants-in-Aid for Scientific Research (No. 20390462) from the Ministry of Education, Culture, Sports, Science and Technology in Japan, and by the Industrial Technology Research Grant Program from New Energy and Industrial Technology Development Organization (NEDO) of Japan.

References

1. Yoshimura N, Yamaguchi M, Ohashi H, Oshima Y, Oka S, Yoshida M, Murakami H, Tei T (2003) Pulmonary atresia with intact ventricular septum: strategy based on right ventricular morphology. J Thorac Cardiovasc Surg 126:1417–1426
2. Chowdhury UK, Airan B, Talwar S, Kothari SS, Saxena A, Singh R, Subramaniam GK, Juneja R, Pradeep KK, Sathia S, Venugopal P (2005) One and one-half ventricle repair: results and concerns. Ann Thorac Surg 80:2293–2300
3. Hanley FL (1999) The one and a half ventricle repair-we can do it, but should we do it? J Thorac Cardiovasc Surg 117:659–661
4. Uemura H, Yagihara T, Adachi I, Kagisaki K, Shikata F (2007) Conversion to total cavopulmonary connection after failed one and one-half ventricular repair. Ann Thorac Surg 84:666–668
5. Numata S, Uemura H, Yagihara T, Kagisaki K, Takahashi M, Ohuchi H (2003) Long-term functional results of the one and one half ventricular repair for the spectrum of patients with pulmonary atresia/stenosis with intact ventricular septum. Eur J Cardiothorac Surg 24:516–520
6. Freedom RM (1998) Pulmonary atresia with intact ventricular septum—the significance of the coronary arterial circulation. In: Redington AN, Brawn WJ, Deanfield JE, Anderson RH (eds) The right heart in congenital heart disease. Greenwich Medical Media, London
7. Hanley FL, Sade RM, Blackstone EH, Kirklin JW, Freedom RM, Nanda NC (1993) Outcomes in neonatal pulmonary atresia with intact ventricular septum. A multiinstitutional study. J Thorac Cardiovasc Surg 105:406–427
8. Ashburn DA, Blackstone EH, Wells WJ, Jonas RA, Pigula FA, Manning PB, Lofland GK, Williams WG, McCrindle BW, Congenital Heart Surgeons Study members (2004) Determinants of mortality and type of repair in neonates with pulmonary atresia and intact ventricular septum. J Thorac Cardiovasc Surg 127:1000–1007
9. Burkhoff D, Tyberg JV (1993) Why does pulmonary venous pressure rise after onset of LV dysfunction: a theoretical analysis. Am J Physiol 265:H1819–H1828
10. Morley D, Litwak K, Ferber P, Spence P, Dowling R, Meyns B, Griffith B, Burkhoff D (2007) Hemodynamic effects of partial ventricular support in chronic heart failure: results of simulation validated with in vivo data. J Thorac Cardiovasc Surg 133:21–28
11. Goodwin JA, van Meurs WL, Sá Couto CD, Beneken JE, Graves SA (2004) A model for educational simulation of infant cardiovascular physiology. Anesth Analg 99:1655–1664
12. Migliavacca F, Pennati G, Dubini G, Fumero R, Pietrabissa R, Urcelay G, Bove EL, Hsia TY, de Leval MR (2001) Modeling of the Norwood circulation: effects of shunt size, vascular resistances, and heart rate. Am J Physiol Heart Circ Physiol 280:H2076–H2086
13. Santamore WP, Burkhoff D (1991) Hemodynamic consequences of ventricular interaction as assessed by model analysis. Am J Physiol 260:H146–H157
14. Sagawa K, Maughan L, Suga H, Sunagawa K (1988) Cardiovascular interaction. In: Sagawa K, Maughan L, Suga H, Sunagawa K (eds) Cardiac contraction and the pressure–volume relationship. Oxford University Press, Oxford
15. Walther FJ, Siassi B, King J, Wu PY (1986) Blood flow in the ascending and descending aorta in term newborn infants. Early Hum Dev 13:21–25
16. Wang JJ, Flewitt JA, Shrive NG, Parker KH, Tyberg JV (2006) Systemic venous circulation. Waves propagating on a windkessel: relation of arterial and venous windkessels to systemic vascular resistance. Am J Physiol Heart Circ Physiol 290:H154–H162
17. McElhinney DB, Reddy VM, Hanley FL, Moore P (1997) Systemic venous collateral channels causing desaturation after bidirectional cavopulmonary anastomosis: evaluation and management. J Am Coll Cardiol 30:817–824
18. Gatzoulis MA, Shinebourne EA, Redington AN, Rigby ML, Ho SY, Shore DF (1995) Increasing cyanosis early after cavopulmonary connection caused by abnormal systemic venous channels. Br Heart J 73:182–186
19. Webber SA, Horvath P, LeBlanc JG, Slavik Z, Lamb RK, Monro JL, Reich O, Hruda J, Sandor GG, Keeton BR, Salmon AP (1995) Influence of competitive pulmonary blood flow on the bidirectional superior cavopulmonary shunt. A multi-institutional study. Circulation 92:II279–II286
20. Trusler GA, Williams WG, Cohen AJ, Rabinovitch M, Moes CA, Smallhorn JF, Coles JG, Lightfoot NE, Freedom RM (1990) William Glenn lecture. The cavopulmonary shunt. Evolution of a concept. Circulation 82:IV131–IV138
21. Gelatt M, Hamilton RM, McCrindle BW, Gow RM, Williams WG, Trusler GA, Freedom RM (1994) Risk factors for atrial tachyarrhythmias after the Fontan operation. J Am Coll Cardiol 24:1735–1741
22. Balaji S, Gewillig M, Bull C, de Leval MR, Deanfield JE (1991) Arrhythmias after the Fontan procedure. Comparison of total cavopulmonary connection and atriopulmonary connection. Circulation 84:III162–III167
23. Little WC, Ohno M, Kitzman DW, Thomas JD, Cheng CP (1995) Determination of left ventricular chamber stiffness from the time for deceleration of early left ventricular filling. Circulation 92:1933–1939
24. Lisauskas JB, Singh J, Bowman AW, Kovács SJ (2001) Chamber properties from transmitral flow: prediction of average and passive left ventricular diastolic stiffness. J Appl Physiol 91:154–162
25. Garcia MJ, Firstenberg MS, Greenberg NL, Smedira N, Rodriguez L, Prior D, Thomas JD (2001) Estimation of left ventricular operating stiffness from Doppler early filling deceleration time in humans. Am J Physiol Heart Circ Physiol 280:H554–H561
26. Gaynor SL, Maniar HS, Bloch JB, Steendijk P, Moon MR (2005) Right atrial and ventricular adaptation to chronic right ventricular pressure overload. Circulation 112:I212–I218
27. Szabó G, Buhmann V, Graf A, Melnitschuk S, Bährle S, Vahl CF, Hagl S (2003) Ventricular energetics after the Fontan operation: contractility-afterload mismatch. J Thorac Cardiovasc Surg 125:1061–1069

Autonomic Neuroscience: Basic and Clinical 152 (2010) 115–118

Contents lists available at ScienceDirect

Autonomic Neuroscience: Basic and Clinical

journal homepage: www.elsevier.com/locate/autneu

Short communication

In vivo direct monitoring of interstitial norepinephrine levels at the sinoatrial node

Shuji Shimizu [a,c,d,*], Tsuyoshi Akiyama [b], Toru Kawada [a], Toshiaki Shishido [a], Masaki Mizuno [a], Atsunori Kamiya [a], Toji Yamazaki [b], Shunji Sano [c], Masaru Sugimachi [a]

[a] Department of Cardiovascular Dynamics, Advanced Medical Engineering Center, National Cardiovascular Center Research Institute, Osaka, Japan
[b] Department of Cardiac Physiology, National Cardiovascular Center Research Institute, Osaka, Japan
[c] Department of Cardiovascular Surgery, Okayama University Graduate School of Medicine, Dentistry and Pharmaceutical Sciences, Okayama, Japan
[d] Japan Association for the Advancement of Medical Equipment, Tokyo, Japan

ARTICLE INFO

Article history:
Received 1 June 2009
Received in revised form 12 August 2009
Accepted 27 August 2009

Keywords:
Heart rate
Sympathetic nerve terminal activity
Norepinephrine
Sinoatrial node
Microdialysis
Desipramine

ABSTRACT

We assessed in vivo interstitial norepinephrine (NE) levels at the sinoatrial node in rabbits, using microdialysis technique. A dialysis probe was implanted adjacent to the sinoatrial node of an anesthetized rabbit and dialysate was sampled during sympathetic nerve stimulation. Atrial dialysate NE concentration correlated well with heart rate. Desipramine significantly increased dialysate NE concentrations both before and during sympathetic nerve stimulation compared with the absence of desipramine. However, desipramine did not affect the relation between heart rate and dialysate NE concentration. These results suggest that atrial dialysate NE level reflects the relative change of NE concentration in the synaptic cleft. Microdialysis is a powerful tool to assess in vivo interstitial NE levels at the sinoatrial node.

1. Introduction

Heart rate is determined by the frequency of depolarization of sinoatrial (SA) nodal cell during sinus rhythm. The SA node is innervated by sympathetic nerve fibers. These sympathetic nerves, together with parasympathetic nerves, play an important role in the regulation of SA node pacemaker activities. Direct measurement of electrical axonal activity of efferent cardiac sympathetic nerve (Kawada et al., 2004) and indirect measurement of norepinephrine (NE) spillover from plasma NE concentration in the coronary sinus (Meredith et al., 1993) have been used as indices of sympathetic nerve terminal activity on the effector, i.e. sinoatrial node. However, due to the heterogeneity of sympathetic innervation in the heart, quantitative assessment of sympathetic nerve terminal activities on the SA node is essential for better understanding of the sympathetic control of heart rate.

Recently we have developed a microdialysis technique that allows direct monitoring of acetylcholine release into the SA node (Shimizu et al., 2009). In the present study, we monitored interstitial NE levels in the right atrial myocardium adjacent to the SA node using the microdialysis technique and investigated the relation between interstitial NE levels and heart rate in response to sympathetic nerve stimulation. This study may prove the usefulness of microdialysis in assessing the relative change of sympathetic nerve terminal activity on the SA mode.

2. Materials and methods

2.1. Surgical preparation

Animal care was provided in accordance with the *Guiding Principles for the Care and Use of Animals in the Field of Physiological Sciences* approved by the Physiological Society of Japan. All protocols were approved by the Animal Subject Committee of the National Cardiovascular Center. Fourteen Japanese white rabbits weighing 2.4 to 2.8 kg were used in this study. Anesthesia was initiated by an intravenous injection of pentobarbital sodium (50 mg/kg) via the marginal ear vein, and then maintained at an appropriate level by continuous intravenous infusion of α-chloralose and urethane (16 mg/kg/h and 100 mg/kg/h) through a catheter inserted into the femoral vein. The animals were intubated and ventilated mechanically with room air mixed with oxygen. Systemic arterial pressure was monitored by a catheter inserted into the femoral artery. Esophageal temperature, which was measured by a thermometer (CTM-303, Terumo, Japan), was maintained between 38 and 39 °C using a heating pad. Bilateral vagal nerves were exposed through a midline cervical incision and sectioned at the neck.

With the animal in supine position, a full median sternotomy was performed to expose the heart. The right cardiac sympathetic nerve

* Corresponding author. Department of Cardiovascular Dynamics, Advanced Medical Engineering Center, National Cardiovascular Center Research Institute, 5-7-1, Fujishiro-dai, Suita, Osaka, 565-8565, Japan. Tel.: +81 6 6833 5012; fax: +81 6 6835 5403.
E-mail address: shujismz@ri.ncvc.go.jp (S. Shimizu).

1566-0702/$ – see front matter © 2009 Elsevier B.V. All rights reserved.
doi:10.1016/j.autneu.2009.08.017

was exposed through the sternotomy and sectioned intrathoracically. A pair of bipolar stainless steel electrodes was attached to the efferent side of the right cardiac sympathetic nerve. The nerve and electrode were immobilized using a quick-dry silicone gel (Kwik-Cast and Kwik-Sil, World Precision Instruments, Inc., FL, USA). When sympathetic stimulation was required, the efferent sympathetic nerve was stimulated by a digital stimulator (SEN-7203, Nihon Kohden, Japan), at a pulse duration of 1 ms and an amplitude of 5 V. Three stainless electrodes were attached around the incision of sternotomy for the body surface electrocardiogram. The heart rate was determined from the electrocardiogram using a cardiotachometer. Heparin sodium (100 IU/kg) was administered intravenously to prevent blood coagulation. A dialysis probe was implanted and dialysis was conducted as described in *Dialysis Technique* below. At the end of the experiment, the animal was euthanized with an overdose injection of pentobarbital sodium. In the postmortem examination, the right atrial wall was resected with dialysis fiber. We observed the inside of atrial wall macroscopically and confirmed that the dialysis membrane was not exposed to right atrial lumen.

2.2. Dialysis technique

The materials and properties of the dialysis probe have been described previously. (Akiyama et al., 1991; Shimizu et al., 2009) A dialysis fiber of semipermeable membrane (4 mm length, 310 μm outer diameter, 200 μm inner diameter; PAN-1200, 50,000 molecular weight cutoff; Asahi Chemical, Tokyo, Japan) was attached at both ends to polyethylene tubes (25 cm length, 500 μm outer diameter, 200 μm inner diameter). A fine guiding needle (30 mm length, 510 μm outer diameter, 250 μm inner diameter) with a stainless steel rod (5 mm length, 250 μm outer diameter) was used for the implantation of the dialysis probe. A dialysis probe was implanted into the right atrial myocardium near the junction between the superior vena cava and the right atrium. After implantation, the dialysis probe was perfused with Ringer's solution (NaCl 147 mM, KCl 4 mM, $CaCl_2$ 3 mM) at a speed of 2 μl/min, using a microinjection pump (CMA/102, Carnegie Medicin, Sweden). Experimental protocols were started 120 min after implantation of the dialysis probe. We took account of the dead space between the dialysis membrane and the sample tube at the start of each dialysate sampling. Four-μl phosphate buffer (pH 3.5) was transferred into each sample tube before dialysate sampling. Dialysate sampling periods were set at 10 min (1 sample volume = 20 μl). Dialysate NE concentration was analyzed by high performance liquid chromatography (Akiyama et al., 1991).

2.3. Experimental protocols

2.3.1. Protocol 1

To examine whether atrial interstitial NE level reflects NE release from cardiac sympathetic nerve endings, we investigated the effect of sympathetic nerve stimulation on dialysate NE concentration and analyzed the relationship between the dialysate NE concentrations and heart rate ($n = 7$). We sampled control dialysate after transecting the right sympathetic nerve. Then we stimulated the right sympathetic nerve for 10 min each at frequencies of 2, 5 and 10 Hz, and collected the dialysate during each stimulation. There was a 30-min interval between the different stimulation frequencies. Twenty min after sympathetic nerve stimulation, we sampled the dialysate again to check for recovery of NE level.

2.3.2. Protocol 2

Most of the released NE is removed by neuronal uptake mechanism in the heart (Goldstein et al., 1988). To examine whether an increase in atrial interstitial NE level reflects the increase in synaptic NE levels associated with inhibition of neuronal uptake, we investigated the effects of sympathetic nerve stimulation on dialysate NE concentration in the presence of neuronal uptake inhibition and analyzed the relationship between dialysate NE concentration and heart rate ($n = 7$). After intravenous administration of a neuronal uptake inhibitor, desipramine (1.0 mg/kg), we stimulated the right sympathetic nerve and sampled the dialysate in a similar fashion as in Protocol 1.

2.4. Statistical analysis

All data are presented as means ± SE. Heart rate and dialysate NE concentrations (logarithmic transformation) in response to sympathetic stimulation were compared between the absence and presence of desipramine by two-way analysis of variance (ANOVA). If there was not a significant interaction between desipramine and stimulation effects, heart rate and dialysate NE concentrations (logarithmic transformation) in response to sympathetic stimulation were compared using Dunnett's test. After logarithmic transformation of dialysate NE concentration, a linear regression analysis was performed to examine the relation between dialysate NE concentration and heart rate. The differences in slope and intercept between two regression lines were examined. (Glantz, 2005) Differences were considered significant at $P < 0.05$.

3. Results

In Protocol 1 (stimulation alone), right cardiac sympathetic nerve stimulation significantly increased heart rate from 260 ± 8 bpm in the pre-stimulation control to 298 ± 11 bpm during stimulation at 2 Hz ($P < 0.01$ vs. control), 319 ± 10 bpm at 5 Hz ($P < 0.01$ vs. control) and 318 ± 11 bpm at 10 Hz ($P < 0.01$ vs. control) (ANOVA, $P < 0.001$). Heart rate recovered to 261 ± 9 bpm 20 min after stimulation. Right cardiac sympathetic nerve stimulation significantly increased dialysate NE concentration from 0.4 ± 0.1 nM in the pre-stimulation control to 1.0 ± 0.1 nM during stimulation at 2 Hz ($P < 0.01$ vs. control), 2.2 ± 0.5 nM at 5 Hz ($P < 0.01$ vs. control) and 2.9 ± 0.9 nM at 10 Hz ($P < 0.01$ vs. control) (ANOVA, $P < 0.001$). Dialysate NE concentration recovered to the pre-stimulation level 20 min after stimulation (0.6 ± 0.1 nM) (Fig. 1).

In Protocol 2 (desipramine + stimulation), intravenous administration of desipramine significantly increased baseline heart rate (295 ± 11 vs. 263 ± 11 bpm, $P < 0.01$, paired t test) and baseline dialysate NE concentration (1.5 ± 0.2 vs. 0.8 ± 0.2 nM, $P < 0.01$, paired t test) compared

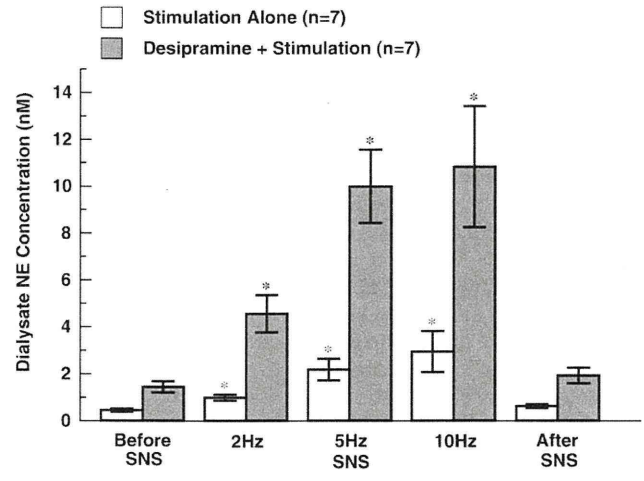

Fig. 1. Dialysate NE concentrations of controls and during electrical stimulation of right cardiac sympathetic nerve at different frequencies. The two-way analysis of variance (ANOVA) revealed the significant effect of sympathetic nerve stimulation on dialysate NE concentration ($P < 0.001$) and the significant difference in dialysate NE concentration ($P < 0.001$) between the absence and presence of desipramine. The interaction between desipramine and stimulation effects was not significant. Values are means ± SE; NE: norepinephrine; SNS: electrical sympathetic nerve stimulation; *n*: number of rabbits; *: $P < 0.01$ vs. the pre-stimulation control by Dunnett's test.

to Protocol 1. Right cardiac sympathetic nerve stimulation significantly increased heart rate from 295 ± 11 bpm in the pre-stimulation control to 349 ± 9 bpm during stimulation at 2 Hz ($P<0.01$ vs. control), 361 ± 8 bpm at 5 Hz ($P<0.01$ vs. control) and 351 ± 9 bpm at 10 Hz ($P<0.01$ vs. control) (ANOVA, $P<0.001$). Heart rate recovered to 295 ± 13 bpm 20 min after stimulation. Right sympathetic nerve stimulation also increased dialysate NE concentration from 1.5 ± 0.2 nM in the pre-stimulation control to 4.6 ± 0.8 nM during stimulation at 2 Hz ($P<0.01$ vs. control), 10.0 ± 1.6 nM at 5 Hz ($P<0.01$ vs. control) and 10.8 ± 2.6 nM at 10 Hz ($P<0.01$ vs. control) (ANOVA, $P<0.001$). Dialysate NE concentration recovered to the pre-stimulation level 20 min after stimulation (1.9 ± 0.3 nM) (Fig. 1). Heart rate and dialysate NE concentrations in Protocol 2 (desipramine + stimulation) were significantly higher than those in Protocol 1 (stimulation alone) (ANOVA, $P<0.001$). The interaction between desipramine and stimulation effects was not significant.

The relation between heart rate and dialysate NE concentration is shown in Fig. 2. Dialysate NE concentration correlated well with heart rate in both Protocols 1 and 2 (Protocol 1: $HR = 290 + 87 \times \log[NE(nM)]$, $R^2 = 0.71$; Protocol 2: $HR = 283 + 74 \times \log[NE(nM)]$, $R^2 = 0.70$) There was no significant difference in the intercept or slope between the two regression lines obtained from Protocols 1 and 2. (Glantz, 2005)

4. Discussion

We were able to monitor in vivo interstitial NE levels at the SA node using microdialysis technique. A neuronal uptake inhibitor, desipramine, significantly increased dialysate NE concentration in the right atrial myocardium. However, desipramine scarcely affected the relation between interstitial NE levels and heart rate.

4.1. Characteristics of dialysate NE concentration in right atrial myocardium

Dialysate NE concentration in the right atrial myocardium increased in response to electrical stimulation of the right cardiac sympathetic nerve and decreased to the pre-stimulation level after stimulation. These results indicate that atrial dialysate NE concentration reflects NE release from cardiac sympathetic nerve endings innervating the right atrium. Furthermore, a semi-log plot demonstrated a linear relationship between the right atrial dialysate NE concentration and heart rate. Judging from this relation, a 10-fold increase in dialysate NE concentration corresponds to an increase in heart rate of 87 bpm. The relative changes in NE release monitored by microdialysis correlate well with the frequency in depolarization of the SA nodal cell. Thus, we consider that dialysate NE concentration does reflect the relative changes in synaptic NE level. The relation between exogenous NE concentration and heart rate has been investigated in the isolated rabbit's atria (Toda, 1969). However, there is no report of a direct method to assess the endogenous NE release into the SA node. Microdialysis enables the monitoring of endogenous NE release into the SA node.

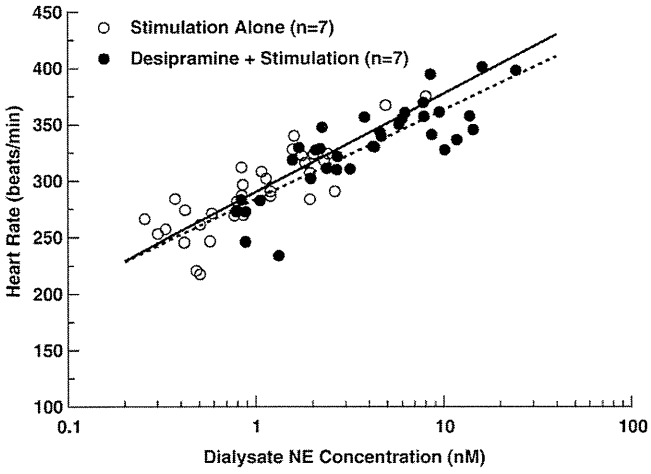

Fig. 2. Relation between dialysate NE concentration (logarithmic scale) and heart rate. Dialysate NE concentration in the right atrial myocardium correlates well with heart rate. Solid line: regression line fitting 35 data points obtained from Protocol 1 (stimulation alone) ($R^2 = 0.71$); dotted line: regression line fitting 35 data points obtained from Protocol 2 (desipramine + stimulation) ($R^2 = 0.70$). NE: norepinephrine.

4.2. Effect of neuronal uptake on dialysate NE concentration

In the presence of desipramine, a neuronal uptake inhibitor, dialysate NE concentration also increased in response to sympathetic nerve stimulation and decreased to the pre-stimulation levels after stimulation. However, dialysate NE concentrations were 3.1–4.6 times higher than the corresponding values in the absence of desipramine. These results are consistent with earlier experimental studies demonstrating that a large part of released NE is removed by neuronal uptake (Goldstein et al., 1988). In the present study, we were able to monitor the change in neuronal NE uptake function induced by desipramine using microdialysis technique.

Linked with the increase in dialysate NE concentrations in the presence of desipramine, heart rates were 33–51 bpm higher than the corresponding values in the absence of desipramine. Thus, desipramine does not alter the relation between dialysate NE concentration and heart rate. The intercept and the slope of regression line also did not differ significantly in the presence and absence of desipramine. These results indicate that neuronal uptake removes effective NE from the synaptic cleft without affecting the sensitivity of the SA nodal cell, and that neuronal NE uptake function plays an important role in the regulation of heart rate. The increase in synaptic NE concentration induced by inhibition of neuronal uptake affects the frequency of depolarization of the SA nodal cell.

Endoh (1975) reported that desipramine shifted the dose–response curve for exogenous NE to the lower NE levels. Since desipramine suppresses the neuronal uptake of both endogenous and exogenous NE, the increase in effective NE on the sinoatrial node may yield this apparent shift in the dose–response curve. Our results suggest that desipramine-inhibited neuronal uptake scarcely affects the relation between synaptic NE concentration and heart rate. Therefore, microdialysis may be a powerful tool to assess the change of synaptic NE concentration in the SA node.

4.3. Limitation

There were several limitations in the present study. First, since we did not section the left cardiac sympathetic nerve, the influence of left sympathetic nerve on the dialysate NE concentration cannot be excluded. Therefore, intravenous administration of desipramine could inhibit neuronal NE uptake at the left sympathetic nerve endings and increase dialysate NE concentration. Second, desipramine may affect the dynamic response of heart rate to sympathetic activation. We have already reported that desipramine decreases the natural frequency of the transfer function from sympathetic nerve activity to heart rate (Kawada et al., 2004). However, cardiac microdialysis using shorter dialysis fiber requires 10-min sampling time to detect changes in myocardial interstitial NE levels. Therefore, we were not able to investigate the dynamic response of heart rate to sympathetic activation in this study.

4.4. Conclusion

We were able to monitor endogenous NE release into the SA node and detect the changes in neuronal uptake function using microdialysis technique. Neuronal NE uptake together with NE release functions play

an important role in the regulation of synaptic NE concentration in the SA node. Microdialysis is a powerful tool to assess the changes of synaptic NE concentration in the SA node.

Acknowledgements

This study was supported by Health and Labor Sciences Research Grants (H18-nano-Ippan-003, H19-nano-Ippan-009, H20-katsudo-Shitei-007 and H21-nano-Ippan-005) from the Ministry of Health, Labor and Welfare of Japan, by Grants-in-Aid for Scientific Research (No. 20390462) from the Ministry of Education, Culture, Sports, Science and Technology in Japan and by the Industrial Technology Research Grant Program from New Energy and Industrial Technology Development Organization (NEDO) of Japan.

References

Akiyama, T., Yamazaki, T., Ninomiya, I., 1991. In vivo monitoring of myocardial interstitial norepinephrine by dialysis technique. Am. J. Physiol. 261, H1643–H1647.

Endoh, M., 1975. Effects of dopamine on sinus rate and ventricular contractile force of the dog heart in vitro and in vivo. Br. J. Pharmacol. 55, 475–486.

Glantz, S.A., 2005. Primer of Biostatistics, 6th ed. McGraw-Hill, New York.

Goldstein, D.S., Brush Jr., J.E., Eisenhofer, G., Stull, R., Esler, M., 1988. In vivo measurement of neuronal uptake of norepinephrine in the human heart. Circulation 78, 41–48.

Kawada, T., Miyamoto, T., Uemura, K., Kashihara, K., Kamiya, A., Sugimachi, M., Sunagawa, K., 2004. Effects of neuronal norepinephrine uptake blockade on baroreflex neural and peripheral arc transfer characteristics. Am. J. Physiol. Regul. Integr. Comp. Physiol. 286, R1110–R1120.

Meredith, I.T., Eisenhofer, G., Lambert, G.W., Dewar, E.M., Jennings, G.L., Esler, M.D., 1993. Cardiac sympathetic nervous activity in congestive heart failure. Evidence for increased neuronal norepinephrine release and preserved neuronal uptake. Circulation 88, 136–145.

Shimizu, S., Akiyama, T., Kawada, T., Shishido, T., Yamazaki, T., Kamiya, A., Mizuno, M., Sano, S., Sugimachi, M., 2009. In vivo direct monitoring of vagal acetylcholine release to the sinoatrial node. Auton. Neurosci. 148, 44–49.

Toda, N., 1969. Interactions of ouabain and noradrenaline in isolated rabbit's atria. Br. J. Pharmacol. 36, 393–408.

Neurochemistry International xxx (2009) xxx–xxx

Contents lists available at ScienceDirect

Neurochemistry International

journal homepage: www.elsevier.com/locate/neuint

Role of Ca^{2+}-activated K^+ channels in catecholamine release from *in vivo* rat adrenal medulla

Tsuyoshi Akiyama [a,*], Toji Yamazaki [a], Toru Kawada [b], Shuji Shimizu [b], Masaru Sugimachi [b], Mikiyasu Shirai [a]

[a] *Department of Cardiac Physiology, National Cardiovascular Center Research Institute, 5-7-1 Fujishiro-dai, Suita, 565-8565 Osaka, Japan*
[b] *Department of Cardiovascular Dynamics, National Cardiovascular Center Research Institute, Suita, 565-8565, Japan*

ARTICLE INFO

Article history:
Received 24 September 2009
Received in revised form 21 October 2009
Accepted 28 October 2009
Available online xxx

Keywords:
Anesthetized rats
Microdialysis technique
Acetylcholine
Norepinephrine
Epinephrine
Ca^{2+}-activated K^+ channels

ABSTRACT

To elucidate the role of Ca^{2+}-activated K^+ (K_{Ca}) channels in the presynaptic acetylcholine (ACh) release from splanchnic nerve endings and the postsynaptic catecholamine release from chromaffin cells, we applied microdialysis technique to the left adrenal medulla of anesthetized rats and investigated the effects of local administration of K_{Ca} channel antagonists through dialysis probes on the release of ACh and/or catecholamine, induced by electrical stimulation of splanchnic nerves or local administration of ACh through the dialysis probes. *Nerve stimulation-induced release*: in the presence of a cholinesterase inhibitor, neostigmine, large-conductance K_{Ca} (BK) channel antagonists, iberiotoxin and paxilline enhanced the presynaptic ACh release and postsynaptic norepinephrine (NE) and epinephrine (Epi) release. Small-conductance K_{Ca} (SK) channel antagonists, apamin and scyllatoxin enhanced the Epi release without any changes in ACh or NE release. In the absence of neostigmine, ACh release was not detected. Iberiotoxin and paxilline enhanced NE and Epi release. Apamin and scyllatoxin had no effect on NE or Epi release. *Exogenous ACh-induced release*: iberiotoxin and paxilline enhanced the Epi release, but had no effect on the NE release. Apamin and scyllatoxin enhanced both NE and Epi release. In conclusion, BK channels on splanchnic nerve endings play an inhibitory role in the physiological catecholamine release from adrenal medulla by limiting presynaptic ACh release while SK channels do not. BK channels on Epi-storing cells may play an inhibitory role in nerve stimulation-induced Epi release. SK channels on NE- and Epi-storing cells play a minor role in nerve stimulation-induced catecholamine release.

1. Introduction

The physiological release of catecholamine from adrenal medulla is controlled by central sympathetic neurons through splanchnic nerves. Splanchnic nerve endings make synaptic-like contacts with chromaffin cells (Coupland, 1965). Activation of splanchnic nerve endings causes Ca^{2+} influx through voltage-dependent Ca^{2+} channels, which evokes exocytotic acetylcholine (ACh) release. This ACh release activates cholinergic receptors on chromaffin cells, which causes Ca^{2+} influx through voltage-dependent Ca^{2+} channels and evokes exocytotic catecholamine release from chromaffin cells (García et al., 2006).

Ca^{2+}-activated K^+ (K_{Ca}) currents are consistently found at neuronal cells or nerve terminals (Meir et al., 1999). K_{Ca} channels are located in the vicinity of voltage-dependent Ca^{2+} channels and activated by Ca^{2+} influx through voltage-dependent Ca^{2+} channels. Activation of the K_{Ca} channels induces outward efflux of K^+, causes hyperpolarization of the membrane, and subsequently limits Ca^{2+} entry through voltage-dependent Ca^{2+}channels. Thus, K_{Ca} channels may be present at two different sites in the adrenal medulla: splanchnic nerve endings and chromaffin cells, and are then involved in the physiological regulation of presynaptic ACh release and/or postsynaptic catecholamine release. In fact, it has been reported that K_{Ca} channels on chromaffin cells play an important role in catecholamine release (Montiel et al., 1995; Uceda et al., 1992; Wada et al., 1995). Little information is, however, available on the role of K_{Ca} channels in the presynaptic ACh release from splanchnic nerve endings.

We have recently developed a dialysis technique to simultaneously monitor the release of presynaptic ACh and postsynaptic catecholamine in the *in vivo* adrenal medulla (Akiyama et al., 2004a). This method makes it possible to investigate the functional roles of K_{Ca} channels in the ACh release from splanchnic nerve endings and the catecholamine release from adrenal medulla in the *in vivo* state. In the present study, we applied the microdialysis technique to the adrenal medulla of anesthetized rats and investigated the effects of K_{Ca} channel antagonists on the release of presynaptic ACh and postsynaptic catecholamine.

* Corresponding author. Tel.: +81 6 6833 5012x2380; fax: +81 6 6872 8092.
E-mail address: takiyama@ri.ncvc.go.jp (T. Akiyama).

0197-0186/$ – see front matter © 2009 Elsevier Ltd. All rights reserved.
doi:10.1016/j.neuint.2009.10.010

In electrophysiological studies, K_{Ca} channels can be divided into two types based on their single channel conductance: large-conductance (BK) and small-conductance K_{Ca} (SK) channels (Blatz and Magleby, 1987). We tested two types of BK channel antagonists: the selective peptidergic BK channel antagonist, iberiotoxin (Candia et al., 1992) and the non-peptidergic BK channel antagonist, paxilline (Kanus et al., 1994). Similarly we tested two types of SK channel antagonists: the selective peptidergic SK channel antagonist, apamin (Blatz and Magleby, 1986) and the selective peptidergic SK channel antagonist different in amino acid sequence, scyllatoxin (Auguste et al., 1990).

2. Materials and methods

2.1. Animal preparation

Animal care was provided in strict accordance with the *Guiding Principles for the Care and Use of Animals in the Field of Physiological Sciences* approved by the Physiological Society of Japan. All protocols were approved by the Animal Subject Committee of the National Cardiovascular Center. Adult male Wistar rats weighing 380–460 g were anesthetized with pentobarbital sodium (50–55 mg/kg, i.p.). A cervical midline incision was made to expose the trachea, which was then cannulated. The rats were ventilated with a constant-volume respirator using room air mixed with oxygen. The left femoral artery and vein were cannulated for monitoring arterial blood pressure and administration of anesthetic, respectively. The level of anesthesia was maintained with a continuous intravenous infusion of pentobarbital sodium (15–25 mg/kg/h, i.v.). The electrocardiogram was monitored to record the heart rate. A thermostatic heating pad was used to keep the esophageal temperature within a range of 37–38 °C. With the animal in the lateral position, the left adrenal gland and left splanchnic nerve were exposed by a subcostal flank incision, and the left splanchnic nerve was transected. In protocols requiring nerve stimulation, shielded bipolar stainless steel electrodes were applied to the distal end of the nerve, which was then stimulated with a digital stimulator (SEN-7203, Nihon Kohden, Japan) with a rectangular pulse (10 V and 1 ms in duration).

2.2. Dialysis technique

Dialysis probe construction was the same as that used in our previous dialysis experiments (Akiyama et al., 2003, 2004a,b). Each end of a dialysis fiber (0.32 mm OD, and 0.25 mm ID; PAN-DX 100,000 mol wt 100% cutoff, Asahi Chemical, Japan) was inserted into a polyethylene tube (25 cm length, 0.5 mm OD, and 0.2 mm ID; SP-8) and glued. The length of the dialysis fiber exposed was 3 mm. At a perfusion speed of 10 μl/min, *in vitro* recovery rates of ACh, norepinephrine (NE) and epinephrine (Epi) were (%): 3.21 ± 0.07, 2.68 ± 0.03, and 2.80 ± 0.03, respectively (number of dialysis probes: 3).

The left adrenal gland was gently lifted, and the dialysis probe was implanted in the medulla of the left adrenal gland along the long axis using a fine guiding needle. The dialysis probe was perfused with Ringer's solution or Ringer's solution containing pharmacological agents at a speed of 10 μl/min using a microinjection pump (CMA/100, Carnegie Medicin, Sweden). Ringer's solution consisted of (in mM) 147.0 NaCl, 4.0 KCl, 2.25 $CaCl_2$. All K_{Ca} channel antagonists tested were locally administered by perfusion through the dialysis probe after being dissolved in Ringer's solution. We started the protocols followed by a stabilization period of 3–4 h and sampled dialysate taking the dead space volume between the dialysis membrane and sample tube into account. Dialysate ACh and catecholamine concentrations were separately measured using each high-performance liquid chromatography with electrochemical detection as previously described (Akiyama et al., 2004a,b).

2.3. Experimental protocols

The experiment was performed based on the previous experiment showing that dialysate ACh and/or catecholamine responses were reproducible on repetition of the pharmacological or electrical stimulation (Akiyama et al., 2004a,b). At the end of the experiment, the rats were sacrificed with pentobarbital sodium, and the implant sites were examined. The dialysis probes were confirmed to have been implanted in the adrenal medulla, and no bleeding or necrosis was found macroscopically.

2.4. Protocol 1

We perfused the dialysis probe with Ringer's solution containing a cholinesterase inhibitor, neostigmine (10 μM) and investigated the effects of BK and SK channel antagonists on the nerve stimulation-induced responses of dialysate ACh and catecholamine concentration. The left splanchnic nerves were firstly electrically stimulated for 2 min at 2 Hz. Then, after a 30-min interval, nerves were subjected to a second stimulation for 2 min at 4 Hz. After these control stimulations, local administration of iberiotoxin (1 μM, $n = 7$), paxilline (100 μM, $n = 7$), apamin (10 μM, $n = 7$) or scyllatoxin (2 μM, $n = 7$) was started. Thirty minutes after local administration of K_{Ca} channel antagonists, nerves were stimulated for 2 min at 2 Hz. Next, after a 30-min interval, nerves were stimulated again for 2 min at 4 Hz. Phosphate buffer (pH 3.5, 4 μl) was transferred into each sample tube before dialysate sampling. Two dialysate samples were continuously collected per nerve stimulation: one before and one during stimulation. One sampling period was 2 min (1 sample volume = 20 μl). Half of the dialysate sample was used for the measurement of ACh, and the remaining half for the measurement of NE and Epi.

2.5. Protocol 2

We investigated the effects of K_{Ca} channel antagonists on the nerve stimulation-induced catecholamine release in the absence of neostigmine. Like in protocol 1, the left splanchnic nerves were stimulated before and 30 min after administration of iberiotoxin ($n = 7$), paxilline ($n = 7$), apamin ($n = 7$) or scyllatoxin ($n = 7$) and two dialysate samples were collected per nerve stimulation. The dialysate sample was used for the measurement of NE and Epi.

2.6. Protocol 3

We investigated the effects of K_{Ca} channel antagonists on exogenous ACh-induced catecholamine release. The dialysis probe was perfused with Ringer's solution. ACh (1 mM) was locally administered to the adrenal medulla through the dialysis probe for 1 min. After first administration of ACh, local administration of iberiotoxin (1 μM, $n = 7$), paxilline (100 μM, $n = 7$), apamin (10 μM, $n = 7$) or scyllatoxin (2 μM, $n = 7$) was started. Thirty minutes after local administration of K_{Ca} channel antagonists, ACh (1 mM) was locally administered again for 1 min. Phosphate buffer (pH 3.5, 2 μl) was transferred into each sample tube before dialysate sampling. Two dialysate samples were continuously collected per local administration of ACh: one before and one during administration. One sampling period was 1 min (1 sample volume = 10 μl). The dialysate sample was used for the measurement of NE and Epi.

2.7. Drugs

Drugs were mixed fresh for each experiment. Neostigmine methylsulfate (Shionogi, Japan), iberiotoxin (Peptide Institute, Japan), apamin (Peptide Institute) and scyllatoxin (Peptide Institute) were dissolved and diluted in Ringer's solution. Paxilline (Sigma Chemical, USA) was dissolved in DMSO and diluted in Ringer's solution. The final concentration of DMSO in the working solution was 0.5% (v/v).

2.8. Statistical methods

To examine the effects of nerve stimulation, local administration of ACh, and K_{Ca} channel antagonists, we analyzed heart rate and mean arterial pressure, basal dialysate NE and Epi content, and dialysate ACh, NE and Epi responses, by using one-way analysis of variance with repeated measures. When statistical significance was detected, the Newman–Keuls test was applied (Winer, 1971). Statistical significance was defined as $P < 0.05$. Values are presented as means ± SE.

3. Results

3.1. Changes in heart rate and mean arterial pressure

Local administration of neostigmine, K_{Ca} channel antagonists, and ACh through the dialysis probe did not change basal heart rate or mean arterial pressure. In protocol 1, nerve stimulation increased mean arterial pressure from 113 ± 3 mmHg in control to 131 ± 2 mmHg at 2 Hz ($n = 28$, $P < 0.05$) and 132 ± 2 mmHg at 4 Hz ($n = 28$, $P < 0.05$), and decreased heart rate from 436 ± 4 beats/min in control to 424 ± 4 beats/min at 2 Hz ($n = 28$, $P < 0.05$) and 420 ± 4 beats/min at 4 Hz ($n = 28$, $P < 0.05$). In protocol 2, nerve stimulation increased mean arterial pressure from 115 ± 4 mmHg in control to 129 ± 3 mmHg at 2 Hz ($n = 28$, $P < 0.05$) and 131 ± 3 mmHg at 4 Hz ($n = 28$, $P < 0.05$), and decreased heart rate from 423 ± 3 beats/min in control to 410 ± 4 beats/min at 2 Hz ($n = 28$, $P < 0.05$) and 404 ± 3 beats/min at 4 Hz ($n = 28$, $P < 0.05$). Heart rate and mean arterial pressure recovered to basal levels after nerve stimulation. After administration of K_{Ca} channel antagonists, nerve stimulation evoked the same responses of heart rate and mean arterial pressure.

Please cite this article in press as: Akiyama, T., et al., Role of Ca^{2+}-activated K^+ channels in catecholamine release from *in vivo* rat adrenal medulla. Neurochem. Int. (2009), doi:10.1016/j.neuint.2009.10.010

Table 1
Basal NE and Epi release before and after local administration of K_{Ca} channel antagonists.

	NE (nM)	Epi (nM)
Iberiotoxin ($n=21$)		
Before administration	4.8 ± 0.3	16.7 ± 1.0
After administration	5.0 ± 0.4	21.7 ± 1.6*
Paxilline ($n=21$)		
Before administration	4.7 ± 0.3	15.7 ± 1.1
After administration	4.8 ± 0.4	22.0 ± 1.9*
Apamin ($n=21$)		
Before administration	4.9 ± 0.4	17.1 ± 1.1
After administration	4.6 ± 0.5	21.2 ± 1.6*
Scyllatoxin ($n=21$)		
Before administration	4.9 ± 0.3	15.3 ± 0.7
After administration	5.1 ± 0.4	20.6 ± 0.9*

Values are means ± SE. *n*, no. of rats; NE, norepinephrine; Epi, epinephrine. *$P < 0.05$ vs. values before administration.

3.2. Basal ACh and catecholamine release

ACh could not be detected in dialysate before nerve stimulation even in the presence of neostigmine. In contrast, substantial amounts of NE and Epi were observed in dialysate before nerve stimulation or ACh administration. Local administration of neostigmine did not influence this basal catecholamine release. BK channel antagonists, iberiotoxin and paxilline did not change basal NE release but increased basal Epi release. Similarly, the SK channel antagonists, apamin and scyllatoxin did not change basal NE release, but increased basal Epi release (Table 1).

ACh was detected in dialysate only during nerve stimulation in the presence of neostigmine. Thus, we expressed this detected dialysate ACh concentration as an index of ACh release induced by nerve stimulation. In contrast, we subtracted basal dialysate NE and Epi content before nerve stimulation or ACh administration from those during stimulation or ACh administration, and expressed these subtracted values as indices of NE and Epi release induced by nerve stimulation or ACh administration.

3.3. Effects of K_{Ca} channel antagonists on the nerve stimulation-induced ACh and catecholamine release in the presence of neostigmine

Iberiotoxin enhanced the nerve stimulation-induced release of presynaptic ACh and postsynaptic catecholamine (Fig. 1A). ACh release increased from 4.5 ± 0.8 to 7.4 ± 0.7 nM at 2 Hz and from 9.4 ± 1.0 to 14.0 ± 1.0 nM at 4 Hz. NE release increased from 7 ± 0.5 to 32 ± 3 nM at 2 Hz and from 27 ± 3 to 74 ± 9 nM at 4 Hz. Epi release increased from 39 ± 5 to 78 ± 5 nM at 2 Hz, and from 105 ± 8 to 193 ± 15 nM at 4 Hz. Similarly, paxilline enhanced the nerve stimulation-induced release of ACh and catecholamine (Fig. 1B). ACh release increased from 4.1 ± 0.4 to 5.9 ± 0.5 nM at 2 Hz and from 9.4 ± 0.7 to 13.7 ± 0.9 nM at 4 Hz. NE release increased from 11 ± 2 to 26 ± 4 nM at 2 Hz, from 31 ± 5 to 58 ± 8 nM at 4 Hz. Epi release increased from 41 ± 7 to 77 ± 14 nM at 2 Hz and from 108 ± 14 to 195 ± 17 nM at 4 Hz.

Apamin had no effect on the nerve stimulation-induced release of ACh and NE, but enhanced the nerve stimulation-induced Epi release (Fig. 2A). Epi release increased from 45 ± 3 to 59 ± 4 nM at 2 Hz and from 108 ± 7 to 139 ± 17 nM at 4 Hz. Scyllatoxin had no effect on the nerve stimulation-induced release of ACh and NE either, but enhanced the nerve stimulation-induced Epi release (Fig. 2B). Epi release increased from 37 ± 4 to 50 ± 3 nM at 2 Hz and from 122 ± 5 to 152 ± 12 nM at 4 Hz.

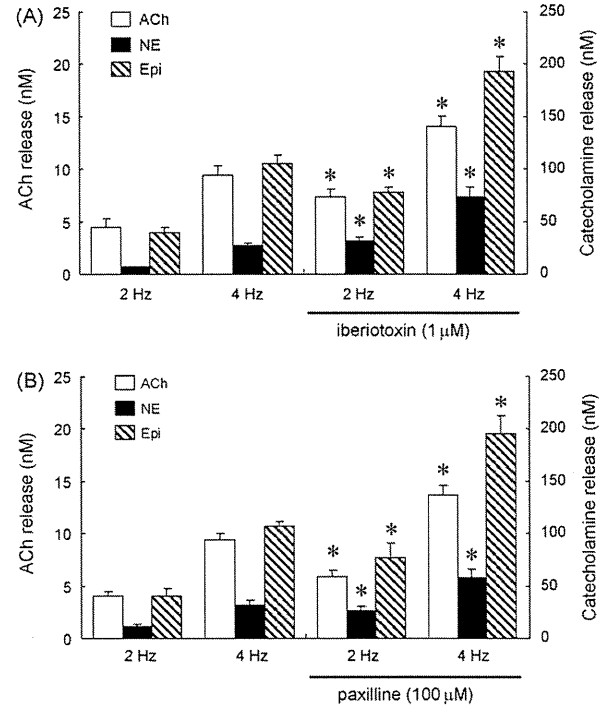

Fig. 1. Effects of BK channel antagonists on the nerve stimulation-induced release of acetylcholine (ACh), norepinephrine (NE) and epinephrine (Epi) in the presence of neostigmine (10 μM): iberiotoxin (A) and paxilline (B) enhanced the release of ACh, NE and Epi at 2 and 4 Hz. Values are means ± SE from seven rats. *$P < 0.05$ vs. ACh, NE or Epi release at the same frequency as before administration of BK channel antagonists.

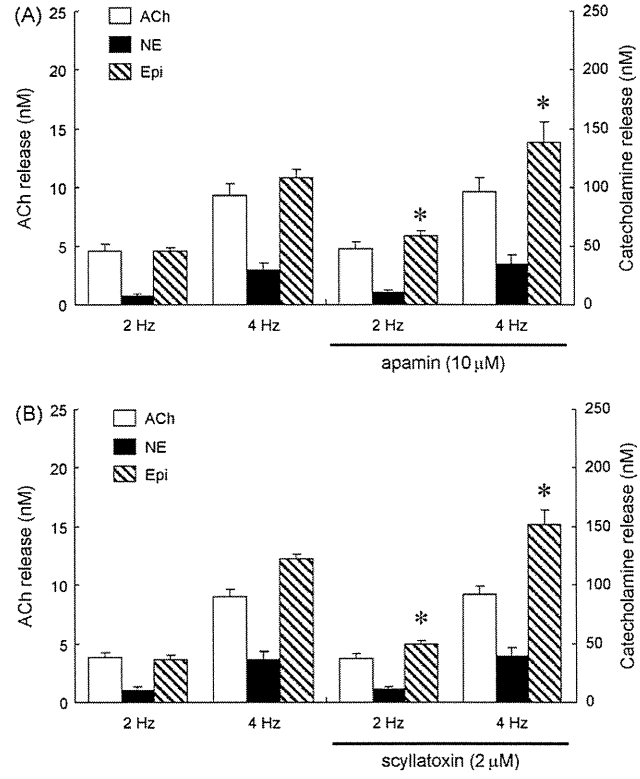

Fig. 2. Effects of SK channel antagonists on the nerve stimulation-induced release of ACh, NE and Epi in the presence of neostigmine (10 μM): apamin (A) and scyllatoxin (B) had no effect on the release of ACh or NE, but enhanced the Epi release at 2 and 4 Hz. Values are means ± SE from seven rats. *$P < 0.05$ vs. ACh, NE or Epi release at the same frequency as before administration of SK channel antagonists.

Please cite this article in press as: Akiyama, T., et al., Role of Ca^{2+}-activated K^+ channels in catecholamine release from *in vivo* rat adrenal medulla. Neurochem. Int. (2009), doi:10.1016/j.neuint.2009.10.010

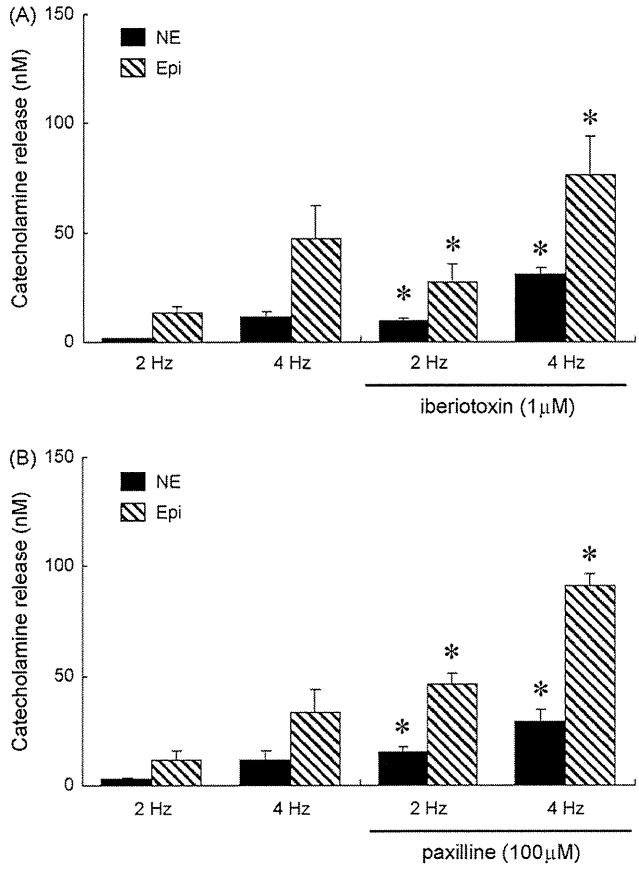

Fig. 3. Effects of BK channel antagonists on the nerve stimulation-induced release of NE and Epi in the absence of neostigmine: iberiotoxin (A) and paxilline (B) enhanced the release of NE and Epi at 2 and 4 Hz. Values are means ± SE from seven rats. *$P < 0.05$ vs. NE or Epi release at the same frequency as before administration of BK channel antagonists.

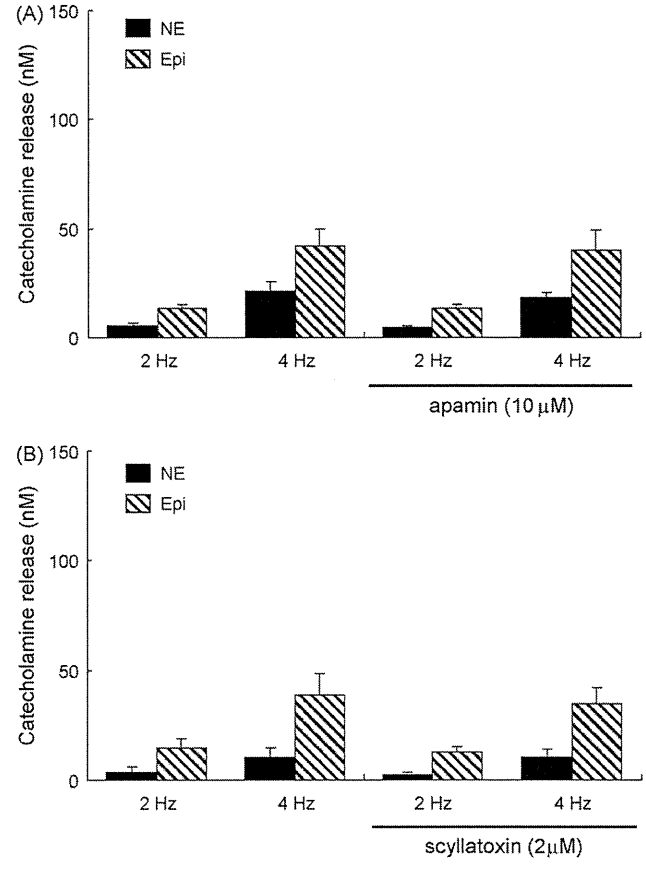

Fig. 4. Effects of SK channel antagonists on the nerve stimulation-induced release of NE and Epi in the absence of neostigmine: apamin (A) and scyllatoxin (B) had no effect on the release of NE or Epi at 2 or 4 Hz. Values are means ± SE from seven rats.

3.4. Effects of K_{Ca} channel antagonists on the nerve stimulation-induced catecholamine release in the absence of neostigmine

Iberiotoxin enhanced the nerve stimulation-induced catecholamine release at both 2 and 4 Hz (Fig. 3A). NE release increased from 2 ± 0.3 to 10 ± 2 nM at 2 Hz and from 12 ± 3 to 31 ± 3 nM at 4 Hz. Epi release increased from 13 ± 3 to 27 ± 9 nM at 2 Hz and from 47 ± 15 to 76 ± 18 nM at 4 Hz. Similarly, paxilline enhanced the nerve stimulation-induced catecholamine release (Fig. 3B). NE release increased from 3 ± 0.6 to 15 ± 2 nM at 2 Hz and from 12 ± 4 to 29 ± 5 nM at 4 Hz. Epi release increased from 12 ± 4 to 46 ± 5 nM at 2 Hz and from 34 ± 10 to 91 ± 6 nM at 4 Hz. Apamin and scyllatoxin had no effect on the nerve stimulation-induced catecholamine release at 2 or 4 Hz (Fig. 4A and B).

3.5. Effects of K_{Ca} channel antagonists on the exogenous ACh-induced catecholamine release

Iberiotoxin had no effect on the exogenous ACh-induced NE release, but enhanced the exogenous ACh-induced Epi release. Epi release increased from 108 ± 11 to 127 ± 10 nM (Fig. 5A). Similarly, paxilline had no effect on the exogenous ACh-induced NE release but enhanced the exogenous ACh-induced Epi release. Epi release increased from 93 ± 5 to 137 ± 13 nM (Fig. 5B). Apamin enhanced the exogenous ACh-induced catecholamine release (Fig. 6A). NE release increased from 37 ± 4 to 49 ± 4 nM and Epi release from 103 ± 8 to 122 ± 9 nM. Similarly scyllatoxin enhanced the exogenous ACh-induced catecholamine release (Fig. 6B). NE release increased from 32 ± 3 to 47 ± 3 nM and Epi release from 108 ± 6 to 140 ± 11 nM.

4. Discussion

4.1. Roles of K_{Ca} channels on splanchnic nerve endings in presynaptic ACh release

We found that, in the *in vivo* adrenal medulla, both iberiotoxin and paxilline enhanced the nerve stimulation-induced release of presynaptic ACh at 2 and 4 Hz by ~50% in the presence of neostigmine (Fig. 1). BK channels currents have been confirmed on cholinergic nerve endings including motor nerves in the neuromuscular junction (Flink and Atchison, 2003), presynaptic nerves in the chick ciliary ganglion (Sun et al., 1999) and tracheal parasympathetic nerves (Zhang et al., 1998). Activation of the K_{Ca} conductance is considered to limit Ca^{2+} entry through voltage-dependent Ca^{2+}channels, and subsequently reduce transmitter release (Meir et al., 1999). Our results strongly suggest that BK channels are present on the splanchnic nerve endings and involved in the control of ACh release. In the perfused cat adrenal gland, charybdotoxin, a BK channel antagonist, enhanced catecholamine release when transmural electrical stimulation was applied at low external Ca^{2+} concentrations, but not when exogenous ACh was administered (Montiel et al., 1995). In the perfused rat adrenal gland, charybdotoxin enhanced the release of Epi and NE induced by transmural electrical stimulation, but not the release induced by administration of ACh (Nagayama et al., 2000b). These indirect studies suggested that BK channels may be involved in the control

Please cite this article in press as: Akiyama, T., et al., Role of Ca^{2+}-activated K^+ channels in catecholamine release from *in vivo* rat adrenal medulla. Neurochem. Int. (2009), doi:10.1016/j.neuint.2009.10.010

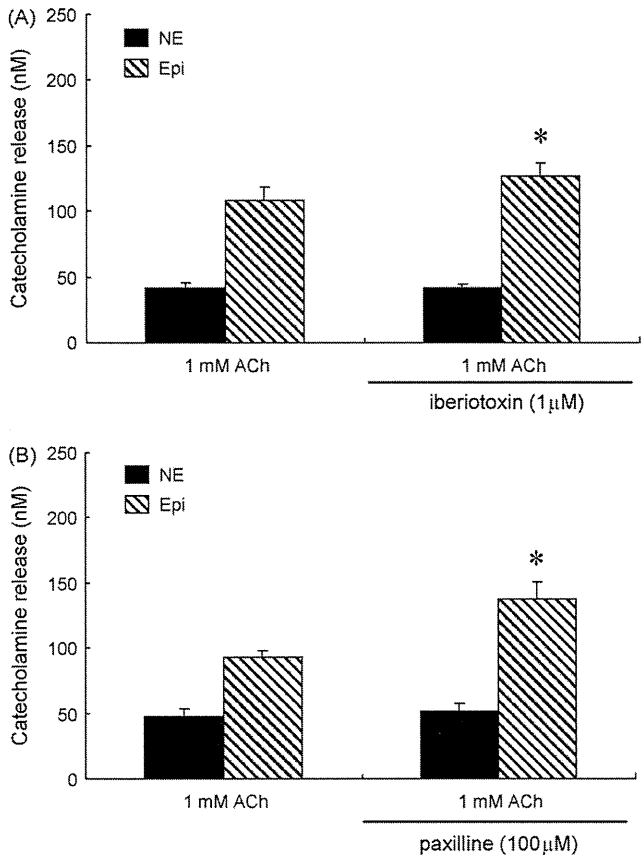

Fig. 5. Effects of BK channel antagonists on the exogenous ACh-induced release of NE and Epi: iberiotoxin (A) and paxilline (B) had no effect on NE release, but enhanced Epi release. Values are means ± SE from seven rats. $^*P < 0.05$ vs. NE or Epi release before administration of BK channel antagonists.

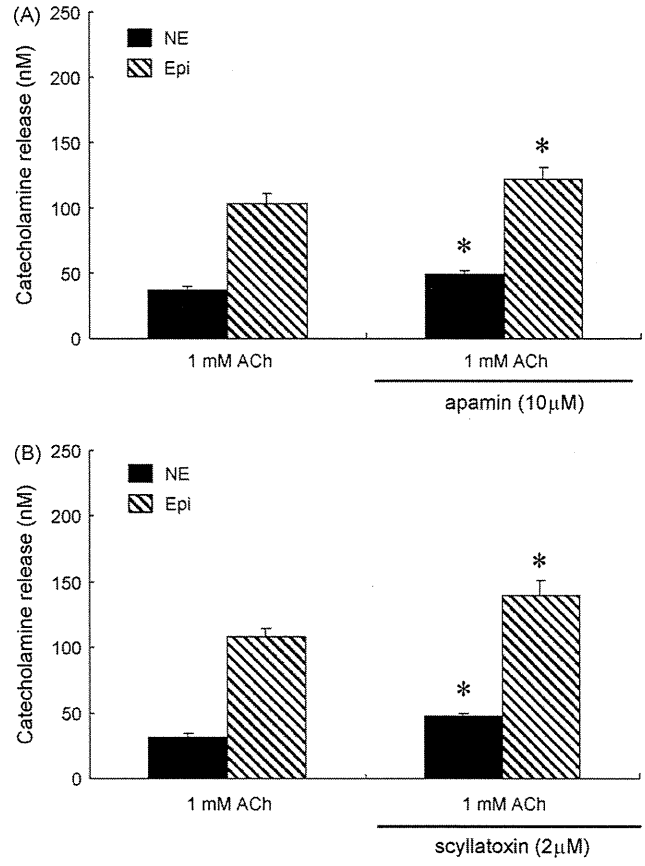

Fig. 6. Effects of SK channel antagonists on the exogenous ACh-induced release of NE and Epi: apamin (A) and scyllatoxin (B) enhanced the release of NE and Epi. Values are means ± SE from seven rats. $^*P < 0.05$ vs. NE or Epi release before administration of SK channel antagonists.

of catecholamine release at the presynaptic site. But there has been no direct study investigating the effect of BK channel antagonists on ACh release from splanchnic nerve endings. This is the first direct study to demonstrate that BK channels are involved in the control of ACh release from splanchnic nerve endings. In the *in vivo* adrenal medulla, we observed a substantial enhancement of ACh release by BK channel antagonists at a frequency of 2 Hz with this degree of enhancement being similar to that at a frequency of 4 Hz (Fig. 1). BK channels on splanchnic nerve endings could be functional under physiological conditions. In our previous study, the nerve stimulation-induced catecholamine release was in large part cholinergic in the presence or absence of neostigmine (Akiyama et al., 2003). Thus, BK channels play an inhibitory role in the physiological catecholamine release from adrenal medulla by limiting presynaptic ACh release.

In contrast to BK channel antagonists, apamin and scyllatoxin had no effect on the nerve stimulation-induced ACh release at 2 or 4 Hz (Fig. 2). In perfused cat adrenal glands preloaded with [^{3}H]-choline, apamin did not modify the efflux of [^{3}H]-labeled compound evoked by transmural electrical stimulation (Montiel et al., 1995). SK channels seem to be absent on splanchnic nerve endings or play a minor role in the ACh release from splanchnic nerve endings.

4.2. Role of K_{Ca} channels on chromaffin cells in catecholamine release

Iberiotoxin and paxilline had no effect on the exogenous ACh-induced NE release, but enhanced exogenous ACh-induced Epi release (Fig. 5). Adrenal chromaffin cells are divided into two populations: NE- and Epi-storing cells (Coupland, 1984). While BK channels seem to be absent on NE-storing cells or play a minor role in the nerve stimulation-induced NE release, BK channels seem to be present on Epi-storing cells. It has been reported that BK channels present at rat chromaffin cells are activated by Ca^{2+} influx and contribute to the rapid termination of action potentials (Prakriya and Lingle, 1999), while iberiotoxin augments the nicotinic receptor-mediated catecholamine secretion from bovine adrenal chromaffin cells (Wada et al., 1995). The enhancement by BK channel antagonists of nerve stimulation-induced Epi release may be in part ascribed to their direct effects on Epi-storing cells. BK channels on Epi-storing cells may be involved in the control of nerve stimulation-induced Epi release. In perfused rat and cat adrenal glands, charybdotoxin, a BK channel antagonist, does not affect the exogenous ACh-induced catecholamine release (Montiel et al., 1995; Nagayama et al., 2000b). Our results of Epi release were inconsistent with these studies, possibly due to differences in the BK channel antagonists used and/or in methodology because charybdotoxin is pharmacologically less selective than iberiotoxin for BK channels (Garcia et al., 1991).

Both apamin and scyllatoxin enhanced the nerve stimulation-induced Epi release in the presence of neostigmine without changes in ACh release (Fig. 2), and the exogenous ACh-induced release of NE and Epi (Fig. 6). These results suggest that SK channels are present on both NE- and Epi-storing cells and that such enhancement is due to the direct effects of SK channel antagonists on chromaffin cells. Neither apamin nor scyllatoxin, however, had any effect on the nerve stimulation-induced NE release in the presence or absence of neostigmine, and the nerve

Please cite this article in press as: Akiyama, T., et al., Role of Ca^{2+}-activated K^+ channels in catecholamine release from *in vivo* rat adrenal medulla. Neurochem. Int. (2009), doi:10.1016/j.neuint.2009.10.010

stimulation-induced Epi release in the absence of neostigmine (Figs. 2 and 4). SK channels on chromaffin cells may play a minor role in the nerve stimulation-induced catecholamine release. It has been reported that SK channels on chromaffin cells are activated by muscarinic receptor stimulation (Nagayama et al., 2000a; Uceda et al., 1992). In our previous study of the same preparation, we demonstrated that muscarinic receptors are present on NE- and Epi-storing cells but play a minor role in the nerve stimulation-induced release of NE and Epi, and that cholinesterase inhibitor elicited muscarinic receptor-mediated Epi release when splanchnic nerve was stimulated (Akiyama et al., 2003). Therefore, SK channels on NE- and Epi-storing cells play an important role in the catecholamine release induced by activation of muscarinic or non-cholinergic receptors including PACAP receptor (Fukushima et al., 2002).

In the perfused rat adrenal gland, apamin enhanced NE release induced by transmural electrical stimulation and a nicotinic receptor agonist (Nagayama et al., 2000b). Therefore, SK channels on NE-storing cells could be activated by nicotinic as well as muscarinic receptors. But, our results of NE release induced by nerve stimulation were inconsistent with this study. In anesthetized dogs, scyllatoxin enhanced catecholamine release induced by a nicotinic receptor agonist but did not affect catecholamine release induced by splanchnic nerve stimulation (Nagayama et al., 1998). Thus, this inconsistency may be due to the difference in the method of nerve stimulation and SK channels on NE-storing cells may be activated by nicotinic receptors in the extrasynaptic region.

4.3. Roles of K_{Ca} channels in basal NE and Epi release

In the present study, substantial basal release of NE and Epi was observed in dialysate before nerve stimulation or ACh administration. Both BK and SK channel antagonists enhanced the basal Epi release but not the basal NE release. In our preparation, splanchnic nerves had been transected before control sampling and basal catecholamine release was not enhanced by a cholinesterase inhibitor, neostigmine. Furthermore, using the same preparation we demonstrated that basal catecholamine release is resistant to not only cholinergic antagonists, but also N-, P/Q-, and L-type Ca^{2+} channel antagonists (Akiyama et al., 2004b). Basal catecholamine release seems to be non-cholinergic and independent of Ca^{2+} influx through voltage-dependent Ca^{2+} channels. Ca^{2+} release from intracellular Ca^{2+} stores may be involved in this basal catecholamine release. It has been suggested in chromaffin cells that K_{Ca} channels on the cell surface are activated by Ca^{2+} release from intracellular Ca^{2+} stores (Ohta et al., 1998). On Epi-storing cells, BK and SK channels may play a role in the Epi release induced by Ca^{2+} release from intracellular Ca^{2+} stores.

4.4. Methodological considerations

Because previous results suggested that distribution across the dialysis membrane is required (Akiyama et al., 2003, 2004a), we used the K_{Ca} channel antagonists at a concentration 10 times higher than that required for complete channel blockade in experimental settings *in vitro*. Then, we tested two different types of selective BK and SK channel antagonists in the present study because higher concentrations of K_{Ca} channel antagonists might induce other pharmacological effects.

Cholinesterase inhibitor was necessary to monitor endogenous ACh even during the splanchnic nerve stimulation because released ACh is rapidly degraded by acetylcholinesterase before reaching the dialysis fiber. Then, we examined the effects of K_{Ca} channel antagonists in the presence or absence of neostigmine because neostigmine may influence the effects of K_{Ca} channel antagonists. Local administration of neostigmine enhanced the nerve stimulation-induced catecholamine release to about 2-fold before and after administration of K_{Ca} channel antagonists (Figs. 1 and 3). This enhancement could be due to the elevation of synaptic ACh levels by inhibition of acetylcholinesterase.

5. Conclusion

We applied dialysis technique to the adrenal medulla of anesthetized rats and investigated the effects of K_{Ca} channel antagonists on the presynaptic ACh release from splanchnic nerve endings and the postsynaptic catecholamine release from chromaffin cells. BK channels on presynaptic splanchnic nerve endings play an inhibitory role in the physiological catecholamine release from adrenal medulla by limiting presynaptic ACh release while SK channels do not. BK channels on Epi-storing cells may play an inhibitory role in the nerve stimulation-induced Epi release. SK channels are present on NE- and Epi-storing cells, but play a minor role in the nerve stimulation-induced catecholamine release.

Acknowledgment

This work was supported by a Grant-in-Aid for scientific research (No. 19591829) from the Ministry of Education, Culture, Sports, Science and Technology.

References

Akiyama, T., Yamazaki, T., Mori, H., Sunagawa, K., 2003. Inhibition of cholinesterase elicits muscarinic receptor-mediated synaptic transmission in the rat adrenal medulla. Auton. Neurosci. 107, 65–73.
Akiyama, T., Yamazaki, T., Mori, H., Sunagawa, K., 2004a. Simultaneous monitoring of acetylcholine and catecholamine release in the in vivo rat adrenal medulla. Neurochem. Int. 44, 497–503.
Akiyama, T., Yamazaki, T., Mori, H., Sunagawa, K., 2004b. Effects of Ca^{2+} channel antagonists on acetylcholine and catecholamine releases in the in vivo rat adrenal medulla. Am. J. Physiol. 287, R161–R166.
Auguste, P., Hugues, M., Gravé, B., Gesquière, J.C., Maes, P., Tartar, A., Romey, G., Schweitz, H., Lazdunski, M., 1990. Leiurotoxin I (scyllatoxin), a peptide ligand for Ca^{2+}-activated K^+ channels. J. Biol. Chem. 265, 4753–4759.
Blatz, A., Magleby, K.L., 1986. Single apamin-blocked Ca-activated K^+ channels of small conductance in cultured rat skeletal muscle. Nature 323, 718–720.
Blatz, A., Magleby, K.L., 1987. Calcium-activated potassium channels. Trends. Neurosci. 10, 463–467.
Candia, S., Garcia, M.L., Latorre, R., 1992. Mode of action of iberiotoxin, a potent blocker of the large conductance Ca^{2+}-activated K^+ channel. Biophys. J. 63, 583–590.
Coupland, R.E., 1965. The Natural History of the Chromaffin Cell. Longmans, London.
Coupland, R.E., 1984. Ultrastructural features of the mammalian adrenal medulla. In: Motta, P.M. (Ed.), Ultrastructure of Endocrine Cells and Tissues. Nijhoff, Boston, MA, pp. 168–179.
Flink, M.T., Atchison, W.D., 2003. Iberiotoxin-induced block of Ca^{2+}-activated K^+ channels induces dihydropyridine sensitivity of ACh release from mammalian motor nerve terminals. J. Pharmacol. Exp. Ther. 305, 646–652.
Fukushima, Y., Nagayama, T., Hikichi, H., Mizukami, K., Yoshida, M., Suzuki-Kusaba, M., Hisa, H., Kimura, T., Satoh, S., 2002. Role of K^+ channels in the PACAP-induced catecholamine secretion from the rat adrenal gland. Eur. J. Pharmacol. 437, 69–72.
García, A.G., García-De-Diego, A.M., Gandía, L., Borges, R., García-Sancho, J., 2006. Calcium signaling and exocytosis in adrenal chromaffin cells. Physiol. Rev. 86, 1093–1131.
Garcia, M.L., Galvez, A., Garcia-Calvo, M., King, V.F., Vazquez, J., Kaczorowski, G.J., 1991. Use of toxins to study potassium channels. J. Bioenerg. Biomembr. 23, 615–646.
Kanus, H.G., McManus, O.B., Lee, S.H., Schmalhofer, W.A., Galcia-Calvo, M., Helms, L.M., Sanchez, M., Giangiacomo, K., Reuben, J.P., Smith, A.B., 1994. Tremorgenic indole alkaloids potently inhibit smooth muscle high-conductance calcium-activated potassium channels. Biochemistry 33, 5819–5828.
Meir, A., Ginsburg, S., Butkevich, A., Kachalsky, S.G., Kaiserman, I., Ahdut, R., Demirgoren, S., Rahamimoff, R., 1999. Ion channels in presynaptic nerve terminals and control of transmitter release. Physiol. Rev. 79, 1019–1088.
Montiel, C., López, M.G., Sánchez-García, P., Maroto, R., Zapater, P., García, A.G., 1995. Contribution of SK and BK channels in the control of catecholamine release by electrical stimulation of the cat adrenal gland. J. Physiol. 486, 427–437.

Please cite this article in press as: Akiyama, T., et al., Role of Ca^{2+}-activated K^+ channels in catecholamine release from *in vivo* rat adrenal medulla. Neurochem. Int. (2009), doi:10.1016/j.neuint.2009.10.010